Sudan University of Science and Technology
College of Graduate Studies

Determination of Optical and Structural Properties for a Semiconductor Marital Manufactured from Gum Arabic Doping by Iodine

تحديد الخواص الضوئية والتركيبية لمادة شبه موصله تم تركيبها من الصمغ العربي المشوب باليود

A thesis Submitted for Fulfillment of Requirements for Degree of
Doctor of Philosophy in Physics

By
Halima Mustafa Eltayeb Osman

Supervisor
Elobaid Mohammed Dr. Rawia Abdelgani

March 2022

Holy Verse

بسم الله الرحمن الرحيم

قال تعالى ﴿ وَآيَةٌ لَهُمُ الْأَرْضُ الْمَيْتَةُ أَحْيَيْنَاهَا وَأَخْرَجْنَا مِنْهَا حَبًّا فَمِنْهُ يَأْكُلُونَ (33) وَجَعَلْنَا فِيهَا جَنَّاتٍ مِنْ نَخِيلٍ وَأَعْنَابٍ وَفَجَّرْنَا فِيهَا مِنَ الْعُيُونِ (34) لِيَأْكُلُوا مِنْ ثَمَرِهِ وَمَا عَمِلَتْهُ أَيْدِيهِمْ أَفَلَا يَشْكُرُونَ (35) سُبْحَانَ الَّذِي خَلَقَ الْأَزْوَاجَ كُلَّهَا مِمَّا تُنْبِتُ الْأَرْضُ وَمِنْ أَنْفُسِهِمْ وَمِمَّا لَا يَعْلَمُونَ (36) ﴾

صدق الله العظيم

سورة يس

Dedication

I dedicate this modest research, to my dear mother, to my father soul, to my brothers and sisters, my friends and colleagues, to students of science the researcher

Acknowledgement

Great thanks firstly to our God for this grace which enable me this study. Deepest thanks directed to my Supervisor:

Dr. Rawia Abdelgani also I thank all people helped me to arrangement in idea of this research, and specially thank to all Grand Staff in since department of physics- Sudan University, I would like to thank my family members who supported and helped me to do this work, my friends, and all the professors they taught us all these years.

Abstract

In this work, Gum Arabic (Talha and Hashaba) Nano-material samples were prepared with different Concentration (0.1, 0.3, 0.5, 0.7 and 0.9) m Molar by doping with Iodine. Optical Properties of Gum Arabic doping by Different Concentration of Iodine measured by using the UV- Spectroscopy min 1240, The Nano crystal size of all samples was measured by XRD technique, and study effect of different concentrations on the particle Size and crystal properties of all samples. The study the effected of different concentration on the optical parameters. For all samples the absorbance increases upon increasing the concentration, while the transmission decreases. The value of Energy band gap (E_g) decreased from (4.420) eV to (4.323) eV. The density increasing by rated 0.5465 mg. Cm^{-3}/molar. Particle Size decreasing by rated 2.41 nm / molar, and d-spacing were decrease molar rated 10^{-10}m / molar. And for FTIR there are found all this band (metal-oxygen vibration at difference positions is due to the different values of metal ion-O^{-2} , C-C stretch and C-C-H bending, O-H bending vibration , C=C stretching and stretching mode of H-O-H bending vibration of free or absorbed water which implies that the hydroxyl groups are retained in ferrites in all samples of Gum Arabic (Talha and Hashaba).

المستخلص

في هذا البحث تم تحضير عينات من المواد النانوية للصمغ العربي (طلح وهشاب) بتراكيز مختلفة (0.1 ، 0.3 ، 0.5 ، 0.7 ، 0.9) مولاري عن طريق تطعيمها باليود. قيست الخواص البصرية للصمغ العربي المطعم باليود باستخدام جهاز مطيافية الأشعة فوق البنفسجية – 1240 المصغر، وقيس حجم الكريستال النانوي للعينات بتقنية جهاز حيود الاشعة السينية (XRD) وتمت دراسة تأثير التراكيز المختلفة على حجم الجسيمات وخصائص الكريستال لجميع العينات وكذلك الخصائص البصرية. ووجد أن الامتصاص يزيد بزيادة التركيز ، بينما يقل الإنتقال. انخفضت قيمة فجوة نطاق الطاقة (على سبيل المثال) من (4.420) فولت إلى (4.323) فولت. تزداد الكثافة بمقدار 0.5465 ملي جرام لكل سنتميتر مكعب وانخفض حجم الجسيمات بمعدل 2.41 لكل ملي مول ، أما المسافة بين الذرات تناقصت بمعدل واحد انجستروم لكل ملي مول .وكانت نتائج التحليل الطيفي الكمي عن طريق مطيافية تحويلات فورير للأشعة تحت الحمراء لكل العينات كالأتي بحيث ظهرت الإهتزازات للزمر التالية (اهتزاز المعدن والأكسجين في مواضع الاختلاف يرجع إلى القيم المختلفة لأيون المعدن 2 -) O ^) ، وتمدد CC وانحناء CCH ، واهتزاز الانحناء OH ، وتمديد C = C وتمديده طريقة اهتزاز الانحناء HOH للمياه الحرة أو الممتصة مما يعني أن مجموعات الهيدروكسيل محتفظ بها في الفريت في جميع عينات الصمغ العربي (طلح وهشاب).

List of Content

Chapter Three

Materials and Methods

Chapter Four

Results and Discussion

List of Tables

List of Figures

CHAPTER ONE

INTRODUCTION

1.1 Preface

Gum Arabic is a natural polymer, play an important role in our day. It is one of the major exported goods from Sudan more than 67% of world product is from Sudan. Gum Arabic has many uses in food stuffs and an adhesive material due to its high viscosity and also used as an additive to make stable suspension mixture for medical surapies, lithography, textiles, paint, inlks, and cosmetic. [Leila, 2006].Gum Arabic is most important commercial poly- saccharides and it is probably the oldest food hydro-colloid in current use. Gum arabic is high molecular weight polymeric compounds, composed maily of carbon core mixed in heterogeneous manner, including some materials in tonic forms as salts of macromolecules have weak conductive properties $\{C^{+2}, Mg^{+2}, K^{+}\}$ [FAO, 1990].Gum arabic is produced from many species of Acacia of African origin [1, 2].

Chemically, A. Senegal gum is an Arabian galactoy protein composed of arabinose {17-34%}, galactose {32- 50%}, rhamnose {n- 16%}, glu carbonic acid {3- 50%} and protein 1, 8- 16%} with an optical rotation of {28° to 32°} [Elassam, 2002]. There are a lot of studies which are done in Gum Arabic but all of them are in normal uses in food stuff and adhesive material. So this study takes a different domain concerning new research in addition to identifying new application of Gum Arabic. This study is considered as continuation of the MSC which has aimed to studying conductive properties of Gum Arabic liquid state. This research is aimed to study the electric, magnetic, and optical properties of Gum Arabic crystals to find out the possibility of new applications for this important natural hydrophilic polymerized carbohydrate like optical sensors, solar cells, and capacitor and semi- conductors [3, 4].

1.2 Objectives of the Study

- The importance of this research comes from the fact modern materials by used Gum Arabic (Talha and Hashaba) and Iodine in different concentration.
- The research problem comes from manufacturing that modern materials on lab. There are also factors concerned with the cost and manufacturing. Thus there is an urgent need to know it.
- The men study problem of this research is to determine doping effects on (optical, constriction and ponding groups) properties of Gum Arabic (Talha and Hashaba) doping by Iodine in different concentration (0.1 , 0.3, 0.5, 0.7 and 0.9) m Molar.

1.3 The Aim of the Work

- The purpose of this work is to synthesis Gum Arabic (Talha and Hashaba) with Iodine in different molars (0.1, 0.3, 0.5, 0.7 and 0.9).
- Make 10 samples of this material five by Talha Gum and other five by Hashaba Gum on different concentrations by rated (0.1 ,0.3,0.5 ,0.7 and 0.9) m Molar.
- Used UV-Spectrometer to study the effected of different molars on the optical prorates like (Absorbance, Reflection, Transmissions, Absorption coefficient Extinction coefficient and Energy band gab).
- Used XRD -Spectrometer to study the effected of different molars on the crystal structure characterized.
- Used Fourier Transform Infrared FTIR- Spectrophotometer to study the effected of different molars on locate the band position**.**

1.4 Thesis Layout

The thesis consists of the five chapters. Chapter one is the Introduction and Chapter two is the theoretical background and literature review. Chapter three consist of method, materials, Chapter four Results and Analysis. Chapter five is concerned with Conclusion and Recommendation

CHAPTER TWO
THEORETICAL BACKGROUND AND LITERATURE REVIEW

2.1 Introduction

The elements and their compounds which aggregate into the solid coble classified as amorphous, poly crystalline single crystalline materials depends on arrangement of atoms in the materials. When the atoms in the materials are arranged in regular manner with a three – dimensional periodicity that extends throughout a given volume the solid, the material is considered to be as crystal. In poly crystalline materials the periodic arrange of atom is interrupted randomly along two dimensional sections that can interest dividing a given volume of solid into a number of smaller single crystalline regions. If, however, there is no periodicity in the arrangement of atom the material is classified as amorphous. Although semi conducting properties are observed in all three classes of solids we restrict our attention to semi conducting materials in single crystalline for doing this. The erotically, when we consider that the spacing between nearest neighbor atoms in a solid is typically several angstroms { 10^{-8} cm} we find this enormous number of atoms were arranged randomly in the material it would be very difficult to construed a useful physically theory of semiconductor behavior [physical properties of semiconductors]. In single crystals however, the theoretical problems are reduced to manageable size and we find that many of the important properties of solids are actually determined by the periodicity of the atoms. Practically the use of single crystal is greatly simplifies a number of the processing steps the high device fields that are characteristic of modern integrated circuit technology. Also charge carriers in device operations, most useful semiconductor devices are fabricated with single crystalline material [5, 6, and 7].

Semiconductor materials at have basically the same structure as insulators filled valence band separated from any empty conduction band by a band gap containing no allowed energy states. The difference ties into size of band gap

^{E}g, which is smeller in semiconductors than in insulators. The relative small band gaps of semiconductors allow for excitations of electrons from the lower valence band to the upper conduction band by reasonable a mounts of thermal or optical energy at the room temperature semiconductors with Eg 1.0ev will have a significant number of electrons excited thermally a cross the energy gap into the conduction band, where as an insulator with Eg ~ 10.0 eV will have an eligible number of such excitations. Thus an important difference between semiconductors and insulators is that the number of electrons available for conduction can be increased greatly in semiconductors by thermal or optical energy. The distinction between insulators and semiconductors is one of degree rather than kind insulator has larger band gaps perhaps 3 eV on more, while semiconductors have band gaps ranging from 2.5 eV down to 0.1 eV. In metals the bands either overlap or one only partially filled thus electrons or empty energy states are intermixed within the bands so that electrons can move freely under the influence of an electric field [5, 6, and 7].

2.2 Simple Lattices

Although no semiconductors crystallize into simple lattice they form the basis for understanding the more complicated semiconductors structure. We will use them to illustrate some of the more important concepts involved in forming a mathematical description of the crystal lattice.

A concept most useful in specifying the underlying geometry of crystal structure is the Bravais Lattice. A Baravais lattice is the infinite matrix of points which, together with the atoms or molecules situated at the points, form the crystal structure it has the property that arrangement of Lattice sites around any given lattice site is the same as that around any other site mathematically, A Bravais Lattice consist of all poivrts generated by the vectors.

$R= \sum n_i, a_i, \qquad i= 1, 2, 3$ **(2.1)**

Where a_i is noncoplanow vectors and n_i take on all integral values. The a_i which generate the Bravais Lattice is known as primitive vectors [8].

In the simple cubic structure, which has an atom at each corner of a cube of dimension the Bravais Lattice can be determined by three mutually orthogonal vectors.

a_1=ax, a_2 =ay, a_3=az

Where x, y, and z are Cartesian unit vectors. This set of vectors demonstrates the basic symmetry of the structure and it is easy to see that the entire Bravais Lattice can be constructed with these vectors this set of primitive vectors is not unique, however, in defining the simple cubic Brava's can also be used to construct the Lattice as well as an infinite number of other sets.

The boy. centrated cubic structure has an atom at each corner of cubic dimension and one at the point determined by the intersection of the cubic body diagonals, another Lattice of interest in semi-conductor crystal structure is the hexagonal close packed Lattice. Although not a Baravais Lattice, because the Lattice sites are not equivalent it consist of two interpenetrating simple hexagonal Lattices which are Bravais Lattice. The simple hexagonal Lattice consist of Lattice site at each corn of an equilateral triangle of side a, with an additional set of points on triangle at a distance above the first [9, 10, and11].

2.3 Crystal Structure

Solids occur in the crystalline or amorphous state. In the crystalline solid about 10^{28} atoms/m3 are arranged in three dimensions in regular manner. This structure may be obtained by repeating in three dimensions an elementary arrangement of some atoms or building blocks called unit cells. Consider the internal structure of crystals in more detail. For it description it is convenient to use the notion of a crystal Lattice one usually distinguishes simple (Brava's) Lattices and Lattices with a basis [9, 10, and11].

To describe a unit cell, we should specify, its three edges a,b and c and three angles α, β, λ between them this six values define the parameters of the cells. One such as contains one atoms. Lattice with a basis can be visualized as two interpenetrating simple sub Lattice one inserted into the other each defined translation vectors a and b [12]

2.3 Optical properties

2.3.1 Electron – photon Interaction

The interaction between an electron and photon

$$E = - \partial A/\partial t \quad (2.2)$$

$$\mu H = \nabla r \chi A \quad (2.3)$$

The vector potential to have the form of plane wave

$$A = \frac{1}{2} A_a \exp [i(qr-\omega t)] + \frac{1}{2} A_a \exp [-i(qr-\omega t)] \quad (2.4)$$

Where a is the unit polarization vector in direction of E and {q} is the wave vector, the wave vector is related to the frequency by

$$|q| = \omega\eta /c \quad (2.5)$$

Where {c} is the velocity of light and {y} is the refractive index of the material.

The energy of photon is simply

$$\zeta = \hbar \omega \quad (2.6)$$

The classical Hamiltonian of an electron with wave vector **k** interacting with a light wave of vector potential A is

$$H = \frac{1}{2m} (\hbar k - q A)^2 \quad (2.7)$$

$$H = \frac{1}{2m} (\hbar^2 k^2 - \hbar q k .A - \hbar q A k + q^2A^2) \quad (2.8)$$

Using the operator form of K

$$H = \frac{1}{2m}(h^2 \nabla r^2 + i2q h A \nabla r + q^2 A^2) \quad (2.9)$$

For low light levels

$$H = - \hbar\nabla r\, 2/2m + (I q \hbar/m) A.\nabla r \quad (2.10)$$

$$H = H_0 + H \quad (2.11)$$

H due to the electron – photon interaction

H_0 unperturbed electron energy.

This interaction can result in change of state for the electron with time it is necessary to solve the time dependent [13, 14, and 15]

Schrodinger equation

$$(H_0 + H) \psi = i \hbar \partial \psi/\partial t \quad (2.12)$$

$\psi = \sum_n A_n(t)\, \psi_n \exp(-1\zeta_n t)/\hbar$ (2.13)

2.4 Optical Prorates

2.4.1 Absorption coefficients

Much of the information about the properties of materials is obtained when they interact with electromagnetic radiation. When a beam of light (photons) is incident on a material, the intensity is expressed by the Lambert-Beer-Bouguer law:

$$I = I_o \exp(-\alpha d) \quad (2.14)$$

If this condition for absorption is met, it appears that the optical intensity of the light wave, (I), is exponentially reduced while traveling through the film. If the power that is coupled into the film is denoted by I0, gives the transmitted intensity that leaves the film of thickness d.

(α) Is called "absorption coefficient". From (2.2) it follows that

$$\alpha = -\frac{1}{d}\, \mathrm{Lin}\left(\frac{I}{I_o}\right) \quad (2.15)$$

It is clear that α must be a strong function of the energy hν of the photons. For hν < Eg (direct), no electron hole pairs can be created, the material is transparent and α is small. For hν ≥ Eg (direct), absorption should be strong. All mechanisms other than the fundamental absorption may add complications (e.g. "sub band gap absorption" through excites), but usually are not very pronounced.

Optical transmission measurements were carried out to determine the film thickness, the wavelength dependence of the refractive index and optical absorption coefficient. The optical constants were determined from the optical transmission measurements using the method described by Swanepoel [16].

The transparent substrate has a thickness several orders of magnitude larger than (d) and has index of refraction (n) and absorption coefficient (α = 0). The index of refraction for air is taken to be n_0 =1. In the transparent region (α =0) the transmission is determined by n and s through multiple reflections. In the

region of weak absorption α is small and the transmission begins to decrease. In the medium absorption region α is large and the transmission decreases mainly due to the effect of α. In the region of strong absorption the transmission decreases drastically due almost exclusively to the influence of α. If the thickness d is uniform, interference effects give rise to the spectrum.

2.4.2 Determination of Band Gaps

The fundamental absorption is related to band-to-band or to exaction transition, which are subjected to certain selection rules [17, 18]. The transitions are classified into several types, according to the band structure of a material. The relation between absorption coefficient and optic band gap for direct transition (k=0) is given by Tauc equation [18]:

$$\sqrt{\alpha h\nu} = B(h\nu - E_g^{opt}) \tag{2.16}$$

And for indirect transition ($k \neq 0$) the relation becomes

$$\alpha(h\omega) \propto \frac{(\hbar\omega - E_{gap})^2}{\hbar\omega} \tag{2.17}$$

From the αhν versus hν one obtains Eg and B parameters. B is also a useful diagnostic of the material since it is inversely proportional to the extent of the tail state (Δ E) at conduction and valance band edges.

2.4.3 Refractive Index

Light that is transmitted into the interior of transparent materials experiences a decrease in velocity, and, as a result, is bent at the interface; this phenomenon is termed refraction. The index of refraction n of a material is defined as the ratio of the velocity in a vacuum c to the velocity in the medium or

$$n = \frac{c}{\upsilon} \tag{2.18}$$

The magnitude of n (or the degree of bending) will depend on the wavelength of the light. This effect is graphically demonstrated by the familiar dispersion or se parathion of a beam of white light into its component colors by a glass prism. Each color is deflected by a different amount as it passes into and out of the glass, which results in the separation of the colors. Not only does the index

of refraction affect the optical path of light, but also, as explained shortly, it influences the fraction of incident light that is reflected at the surface. Just as Equation (2.6) defines the magnitude of c, an equivalent expression gives the velocity of light in a medium as

$$\nu = \frac{1}{\sqrt{c\mu}} \tag{2.19}$$

Where ν and are, respectively, the permittivity and permeability of the particular substance. From Equation (2.6), we have

$$n = \frac{c}{\nu} = \frac{\sqrt{\epsilon\mu}}{\sqrt{\epsilon_o \mu_o}} = \sqrt{\epsilon_r \, \mu_r} \tag{2.20}$$

Where and are the dielectric constant and the relative magnetic permeability, respectively. Because most substances are only slightly magnetic, and

$$n \cong \sqrt{\epsilon_r} \tag{2.21}$$

Thus, for transparent materials, there is a relation between the index of refraction and the dielectric constant [19].

2.4.4 Reflection

When light radiation passes from one medium into another having a different index of refraction, some of the light is scattered at the interface between the two media even if both are transparent. The reflectivity R represents the fraction of the incident light that is reflected at the interface, or

$$R = \frac{I_R}{I_o} \tag{2.22}$$

Where I0 and IR are the intensities of the incident and reflected beams, respectively. If the light is normal (or perpendicular) to the interface, then

$$R = \left(\frac{n_2 - n_1}{n_{2+} n_1}\right)^2 \tag{2.23}$$

Where n1 and n2 are the indices of refraction of the two media. If the incident light is not normal to the interface, R will depend on the angle of incidence. When light is transmitted from a vacuum or air into a solid s, then

$$R = \left(\frac{n_s - 1}{n_s + 1}\right)^2 \quad (2.24)$$

Because the index of refraction of air is very nearly unity. Thus, the higher the index of refraction of the solid, the greater the reflectivity [20].

2.4.5 Absorption

The intensity of the net absorbed radiation is dependent on the character of the medium as well as the path length within. The intensity of transmitted or non-absorbed radiation continuously decreases with distance x that the light traverses:

$$I_T = I_o e^{-\beta x} \quad (2.25)$$

Where is the intensity of the non-reflected incident radiation and ß the absorption Coefficient (in mm-1), is characteristic of the particular material; furthermore, varies with wavelength of the incident radiation. The distance parameter x is measured from the incident surface into the material. Materials that have large values are considered highly absorptive.

2.4.6 Transmission

The phenomena of absorption, reflection, and transmission may be applied to the passage of light through a transparent solid. For an incident beam of intensity I0 that impinges on the front surface of a specimen of thickness l and absorption coefficient, the transmitted intensity at the back face IT is

$$I_T = I_o(1 - R)^2 e^{-\beta l} \quad (2.26)$$

Where R is the reflectance; for this expression, it is assumed that the same medium exists outside both front and back faces. The derivation of Equation (2.12) is left as a homework problem. Thus, the fraction of incident light that is

transmitted through a transparent material depends on the losses that are incurred by absorption and reflection. Again, the sum of the reflectivity R, absorptivity A, and transmissivity T, is unity according to Equation (2.25). Also, each of the variables R, A, and T depends on light wavelength. This is demonstrated the transmission.

2.5 Conductivity

Conductivity (σ), one of the most misunderstood terms in lithographic printing, continues to confuse printers trying to use this control tool.

Gum Arabic in solution and impart its water loving properties to the plates non-image areas, the gum needs to be in an acidic solution between 3.5 PH and 4.5 PH. When metal plates were introduced, first zinc and later aluminum, the surfaces still needed the protection of the gum and acid to remove any oxidation that may occur during downtime, which could cause scrumming gum Arabic become expensive. Therefore, to protect the plate, the synthetic gums merely protected the plate; they did not impart the same hydrophilic properties gum Arabic did. To compensate, the industry began using lower PH ranges or more acidic fountain solution [21, 22]. Conductivity is a useful tool to monitor the level of a particular fountain solution in a particular source of water you then must determine what level is correct for your running conditions. The arbitrary use of conductivity readings means nothing if press performance has not been established, And water well vary from one source to the next so its conductivity also must be considered, any minerals dissolved in water will affect conductivity level, they don't all help the lithographic process. Traditionally, PH was the test relied on the determine fountain solution concentration. Today, however, conductivity testing is recognized as a much more accurate method. Conductivity measurement is a fast and easy test which is more indicative of fountain solution concentration than PH. This is true for all neutral, alkaline, and many acid type solutions. Both conductivity and PH can provide valuable information. The idea of using gum Arabic to maintain the hydrophilic film surface of a metal plate can be credited to Alois senefelder, the inventor of

offset lithography. He discovered that gum Arabic had a great affinity for water. He also discovered that gum Arabic absorbed especially well to plate surface when it reacted with a mild acid (between 3.5 and 4.5). Gum Arabic, however, is still the most effective material for keeping the non- image areas of plate clean. Today there is a trend to move away from the press room mixed solutions and go to a so called '' one- step'' solution. This is a simply fountain solution additive that is comprised of the gum solution, and alcohol substitutes, it is mixed with water at press side or at a central area [23]. The reaction of alkaline ions with an anionic dicarboxylic polyelectrolyte is studied by means of electrical conductivity measurements. The results Show that lithium, sodium and potassium counter –ions interact in very different way with this poly electrolyte. Conductivity is the ability, or power to transmit or conduct an electrical charge. In water or any solution the degree of conductivity is determined by the number of ions present as a result of minerals or other compounds in the water, the high concentration of ions the higher degree of conductivity. Hydrochloric acid has a high ion level and is an excellent conductor of electricity and gives very high conductivity reading, alcohol by the way does' not conduct electrical charges and has zero conductivity. To measure conductivity an electronic (conductivity meter) the unit of measurement for conductivity is expressed as the (ohm $^{-1}$) [24].

The application of an electric field as in conductance experiment, results initially in the movement of the central ion away from the center of the oppositely charged sphere, the distorted ion atmosphere tends to oppose the applied field, and this decreases the current produced by a given applied electric field. Since the icon atmosphere is more important at higher concentration, this decrease becomes more important at higher concentration.

The ionic atmosphere drag depends on the fact that at most does' not instantaneously adjust itself to the new positions of the ion, One way says that the ionic atmosphere has a relaxation time, the second factor that acts decrease the conduction at higher concentration is an enhanced friction to drag that sets

in, when an electric field is applied, The ions of the oppositely charged electrodes. Each ion moves a velocity that depends on a balance between the electric force and the viscous drag. The average velocity and therefore current are concentration dependent, because the ions can be thought of as carrying along with them their many solvating molecules, and at higher concentration an ion seems to swim against the current produced by the oppositely charged solvated ions moving in the opposite direction [25].

2.6 Electrical Conductivity

The electrical current density can be related to the electric field by using ohm's law

$$\mathbf{J_n = \sigma_n \zeta = q \mu_n n \zeta} \quad (2.27)$$

Where

$\sigma_n = q \mu_n n$ is the electrical conductivity, μ n is the electron mobility and n denotes the electron density .The electron drift velocity vd along the direction of the applied electric field. We can write

$$J_n = q_n v \quad (2.28)$$

Where q is the electronic charge

$$vd = \mu_n \zeta \quad (2.29)$$

μ_n is the low field electron drift mobility [26,27]

$$\mu_n = qt/ m^* \quad (2.30)$$

t is the collision time

m* is the electron effective mass

$$\sigma n = qn . \mu_n = q^2.nt/m^* \quad (2.31)$$

2.7 Electronic Thermal conductivity k_n

The electronic thermal conductivity is due to the flow of thermal energy carried by electrons when a temperature gradient appears across a semi-conductor specimen, the electronic thermal conductivity k_n is defined as the thermal flux density per unit temperature gradient and can be expressed by

$$k_n = -Q_x / \zeta T E_x = 0 \quad (2.32)$$

v_x = is the thermal velocity of electrons in x- direction

E_x is the electron energy 28, 29. And 30].

Where Q_x is the thermal flux density given by

$$Q_x = n\, v_x\, E = \int_0^x v_x\, Ef\,(E)_{gn}\,(E) \tag{2.33}$$

Then the Relationship between J_n and Q_x during by

$$J_n = -qn\, v_x = -q \int_0^x v_x\, f\,(E)_{gn}\,(E)\, De \tag{2.34}$$

2.8 The Mechanical Properties of Crystalline Polymer

The viscoelastic properties of crystalline polymers are much more complex, however, and are not amenable to adequate theoretical explanation for three reasons. First, an amorphous polymer is isotropic. This means that models suitable for describing shear stress. Since crystalline polymer are not (so tropic) this universality does not hold and the range of application of any model is severely limited. Second, the homogeneous nature of amorphous polymer ensures that an applied stress is distributed uniformly rough out the system, at least down to very small (dimensions). Finally, a crystalline polymer is a mixture of regions of different degrees of order ranging all the way from completely order crystalline to completely amorphous regions. This change of composition with respect to ordering is the most difficult obstacle to overcome in formulating a theory of the mechanical behavior of crystalline polymers. Even in the simplest cases the necessity of having the mechanical model change continuously with applied stress has led to serious difficulties.(Science and Technology) [31, 32, 33, 34, and 35].

Direct electron transition from a valence band state with wave vector K to a conduction band state with wave vector K the initial and find state for a direct transition are determined by the photon energy {hw} and the energy band structure [36].

$$H_{kk} = i\, q\, \hbar\, A/2mN \int_v \psi^*_k \exp\,(iq.r)\,(\nabla_r)\psi_k\, dt \tag{2.35}$$

Where ψ_K , ψ_K are the wave functions of valence and conduction band state respectively.

Probability in the entire crystal that on electron will make transition from a state with wave vector K to the state with wave vector K is [37, 38, and 39].

$$\left| A_k(t) \right|^2 = 2\pi t/\hbar \, (q\,\bar{A}/2m)^2 \, (a.p_{k\,k^*}) 2\delta(\zeta_k - \zeta_{k^*} - \hbar\omega) \quad (2.36)$$

The total probability for a band – band transition is

$$P = 2V/(2\pi)^3 \int_{\Omega k} \left| Ak(t) \right|^2 f_o(1 - f_o)\, dk \quad (2.37)$$

$$P = \zeta_g + \hbar^2 k^2 / 2mr \quad (2.38)$$

m r is the reduced mass of the electron and hole.

Another factor that controls the fundamental absorption edge is the temperature of the sample. This reflected primarily in the expansion and contraction of the Lattice with temperature and its effect on the energy gap. The temperature dependence of the energy gap varies considerably among semiconductors it is best determined from experimental results.

The energy gap decreases with increasing of temperature although this behavior holds for most semiconductors, for some material the energy gap increases with increasing of temperature [40, 41].

The electric field dependence of the fundamental absorption edge is referred to as the Franz– Kurdish effect. This electro absorption process can be thought of as phantom assisted tunneling through the energy gap. That is the electron wave functions in the valence and conduction band have exponentially decaying amplitude in the energy gap in the presence of an electric field a valence band electron must runnel through a triangular barrier to reach the conduction band.

$$q\,E = \nabla_r \zeta = \zeta_g / t \quad (2.39)$$

t is thickness

$$t = \zeta_g / q\,E \quad (2.40)$$

$$t(\hbar\omega) = (E_g - \hbar\omega)/q\,E \quad (2.41)$$

E in volts / cm $(E_g - \hbar\omega)$ in e v [42, 43]

The outer shell electrons in the atoms of metal are bound rather weakly. In a crystalline solid, atoms arrange themselves so close to each other that valence

electrons acquire the ability to escape from their atoms and move freely about inside the lattice. This electron sharing leads to uniform distribution of electrons in the metal lattice. Bonding originates through the inter - attraction between the positive ions of the lattice and the electron gas, the electron found between ions draw the latter together, balancing out the repulsive forces between ions themselves. Metallic bonding is inherent in typical metals and many inter metallic compounds. The energy of this type of bonding is also high, hundreds of kilojoules per mole. It is weaker than ionic or covalent bonds but stranger than the Van Der Weals type of interaction. Typical lattice for metals are the face - centred cubic fcc the body – central cubic bcc and the hexagonal lattice of dense packing- metals have high conductivity of heat band electricity due to the presence of these free electron also, they exhibit high ductility owing to the character of this type of bonding. Optical opaqueness and high reflectivity of metal are also due to the presence of free electrons [44,45, and 46].

Ionic crystals are composed of an alternating arrangement of positive and negative ions. At high temperature, these crystal ions become mobile such materials characteristically exhibit ionic conductivity. Ionic crystals absorb light strongly in the infrared portion of the light spectrum, owing to the significant interaction of these electromagnetic waves and the charged ions.

This is very stable bonding and the lattice type thus formed is the fcc lattice very similar to the lattice structure of diamond since outer electrons are an essential part of the bonding process. They will not be free as in metal, this type of bond is highly directional, with four neighboring atoms forming asymmetry tetrahedral structure, it is strong band and its importance in the field of electronic stems from the fact that this tetrahedral covalent bond accounts for many of the interesting properties of semiconductors such as silicon and germanium at moderate temperature, thermal energy tends to break some of these bonds, causing the electrons thus freed to contribute to the electrical conductivity of the material [47,48, 49, and 50].

Hydrogen bonding is the most important type of intermolecular attraction. It is important, however, only when hydrogen is bonded to the very electro negative elements, O, F, or N these are the only elements electro negative enough of form polar bonds that leave a positive charge on hydrogen.

Hydrogen bonding, then occurs between a hydrogen atom an electron negative atom {especially} O, N, or F when the hydrogen is covalently bonded to another such atom {O, N, F} thus hydrogen bonds are important when they are of the type $X - H \ldots Y$ [51, 52, and 53]

When both X and Y are highly electro negative, and especially when they are O, N, or F. Hydrogen bonding is a strong inter molecular attractive force molecular, equal to about 10% of the strength of an ordinary covalent bond. Hydrogen bonding therefore affects many physical properties; the boiling point, density, and surface tension of a hydrogen - bonded substance such as water are higher than they would be if there were no hydrogen bonding. Compound such as the hydro carbon molecules, these substances have relatively low boiling points and densities. The boiling point depends on the energy required to cause molecules to "fly away from each other'' into the vapor phase. In the absence of hydrogen bonding {for example, with hydro carbons} the boiling point depends primarily on molecular weight: the higher the molecular weight the higher the boiling point. In hydrogen bonded substance, energy most be supplied to break the hydrogen bonds and cause the molecules to boil away. Thus hydrogen bonding results in higher boiling points .Hydrogen bonding also explains why compounds that contain oxygen or nitrogen atoms are more water soluble than other compounds of similar molecular weight [54, 55, 56, and 57].

2.9 Literature Review

2.9.1 Improving the Properties of Gum Arabic To Act As Semiconductor

This work done by H. Mustafa. In this work the preparation of Gum Arabic by iodine of different concentrations at room temperature) 25oC) and investigated the effect of vaccination of iodine on the distance between atoms and the angles

between them using Easy Scan device. In addition of determination the absorption and energy gap of the treated samples using (UV-VIS) spectroscopy. The conclusion were prepared tablets of gum Arabic and iodine were introduced in easy scan device where it was knowing the distance and angles between the atoms in Gum Taleh highest Distance between atoms was 70.8 nm when the focus 1.52mg and what can be when the distance is less focus. 1.22mg / L In gum Hashab distance increases between atoms then be fixed between (1.2- 2.0) mg / L where 68.3nm then begin increasing. The angles between atoms in Gum Taleh angles between the atoms of the biggest gum Hashab. Were prepared solutions of gum Arabic and iodine concentrations certain were studied gap energy and higher wavelength was him absorbency in Gum Taleh higher wavelength of absorbency is 360nm in gum Hashab 350nm and found that the gap energy affected by a concentration of gum in Gum Taleh when he was the focus of gum 1g was energy gap equal to 3.04 eV and when he was the focus of gum 2g was 3.09eV and when you add 5 ml of distilled water to the gum solution 1 g wigs affected by the energy gap. In Hashab gum when he was the focus of gum 1g was a gap energy 3.04eV When the concentration of gum 2g was energy gap 2.99V eV and when you add 5 ml of distilled water became energy gap 3.1eV where he greater the concentration of gum I said energy gap[58].

2.9.2 Effects of ã-Irradiation on Some Properties of Gum Arabic (Acacia Senegal L)

The study of this work done by SiddigT. Kafi. The mean of this work was The effects of gamma radiation with variable doses on some properties of gum Arabic (Acacia senegal) obtained from Blue Nile State, in Sudan season 2008 were investigated. Doses of 5.5, 6.5, 7.5, 8.5, 9.5, and 10.5 KGy were used respectively for irradiation of gum Arabic samples. The properties studied include the emulsifying stability, viscosity and absorption. It was found that the best emulsifying stability, highest relative viscosity and highest absorbance were obtained with the highest radiation dose (10.5 KGy).Absorbance

increased drastically compared with the control sample (not irradiated sample). Redshift in the peak absorption wavelength was also observed. Change in the colour of irradiated samples occurred from white to red colour. It was concluded that gamma radiation is capable of enhancement of the properties of gum Arabic material. The Conclusion of this study was the properties of gun Arabic (*Acacia senegal*) were studied using variable doses of gamma radiation of 5.5, 6.5, 7.5, 8.5, 9.5, and 10.5 KGy, respectively. It was found that the highest dose of gamma radiation used achieved the best emulsification, viscosity and absorbance. The only drawback is the change of the colour of gum Arabic from white to dark red. This problem needs to be overcome for some applications [59].

2.9.3 Investigating the Electric Conductivity, Magnetic Inductivity, and Optical Properties of Gum Arabic Crystals

Elhadi M. I. Elzain was done this study. In this work Samples of Gum crystals of different thicknesses were prepared by drying Gum solution. A special Capacitor was designed, to be used, for this study. Investigations were carried out with special emphasis on the effects of temperature, crystal thickness, light intensity, upon the desired properties. The maximum value of electric permittivity was 2.8×10-4 C/Nm2.Themaximum value of electric conductivity was 9.88×10-7 ohm-1 cm^{-1}. The results indicated that; Gum Arabic crystals could be considered as weak semiconductors. The light intensity has slight effect on the conductivity, permittivity, and the current passing through the crystals. The results from this study also encourage more researches in this field. The Conclusions and Recommendations of this work was the electrical properties of gum Arabic indicate that; its behavior resembles that of a semiconductor with a large band gap. A new technique based or taking more than 100 readings for (V) and (I) is recommended to be used, to find the values of the energy gap. The magnetic properties of Gum Arabic shows that it is a diamagnetic material. The refractive index is found to be in the range comparable with that of some previous studies. Finally, more researches in this

field are recommended to prove that, Gum Arabic is an industrial material that could find applications with the recent technologies. It is also important to promote experimental techniques necessary to be utilized in such researches, and by using other types of Gums from different places[60].

2.9.4 Assessment of physical properties of gum Arabic from Acacia Senegal varieties in Baringo District, Kenya

This work done by J. K. Lelon . A study was conducted to assess the physical properties of gum arabic obtained from two Acacia senegal varieties (var.senegal and var.kerensis). in Marigat division, Baringo district. Gum arabic samples from the experimental sites at Solit, Kapkun, Kimorok and Maoi were collected, dried and analysed to establish their physical characteristics. Moisture content in gum arabic obtained from variety kerensis in Kimorok and Maoi (17.5 ± 1.00 and 15.4 ± 0.50%) were significantly higher ($P < 0.05$) than those of variety senegal in Solit and Kapkun (15.0 ± 0.50 and 14.9 ± 1.80%), while internal energy (33.4 and 33.76%) were not significantly different ($P > 0.05$) from those of variety senegal found in Kapkun and Solit (33.0 and 32.96%), respectively. Ash content in gum arabic from variety senegal in Solit and Kapkun (2.94 and 3.16%) was higher ($P < 0.05$) than those of variety kerensis found in Kimorok and Maoi (2.88 and 2.72%). In Kapkun, volatile matter in gum arabic from variety senegal (64.2%) was higher ($P < 0.05$) than the quantities of variety kerensis found in Kimorok, Solit and Maoi (63.8, 63.7 and 63.6%), respectively. Moisture content in gum arabic from variety senegal in Solit and Kapkun (15.0 ± 0.40 and 14.9 ± 1.80%) fell within international specifications (13 to 15%), while variety kerensis in Kimorok and Maoi (17.5 and 15.4%) fell outside the specifications. Moisture, ash and volatile matter contents in gum arabic from A. senegal variety senegal were 14.9, 3.16 and 64.24%, while A. senegal variety kerensis had 15.2, 2.88 and 63.8%, respectively. Moisture content in gum arabic from A. senegal variety senegal fell within international specifications while A. senegal variety kerensis fell outside the specifications. Ash, volatile matter and internal energy contents in

gum arabic from A. senegal variety kerensis and variety senegal fell within the specifications. The gum arabic from A. senegal variety senegal in Solit and Kapkun was of better quality than that of A. senegal variety kerensis in Kimorok and Maoi. The conclusion are moisture content in gum arabic from A. senegal variety senegal fell within international specifications while A. senegal variety kerensis fell outside the specifications. Ash, volatile matter and internal energy contents in gum arabic from A. senegal varieties kerensis and senegal fell within the specifications. The gum arabic from A. senegal variety senegal in Solit and Kapkun was of better quality than that of A.senegal variety kerensis in Kimorok and Maoi [61].

2.9.5 Gum Arabic-silver nanoparticles composite as a green anticorrosive formulation for steel corrosion in strong acid media

This work done by Moses M. Solomona . In this study a green anticorrosive composite (GA-AgNPs) has been formulated for steel in 15% HCl and 15% H2SO4 media. Characterization of GA-AgNPs is achieved via FTIR, UV-vis, EDAX, and SEM. Gravimetric, electrochemical (EIS, EFM, DEIS, & TP), and surface assessment (SEM, EDAX, AFM, & XPS) techniques have been deployed in the anticorrosion studies. Results from all applied methods potray GA-AgNPs as effective anticorrosive agent. Inhibition is by adsorption mechanism and follows Langmuir isotherm. GA-AgNPs acts as mixed type inhibitor in 15% H2SO4 solution but as anodic type in 15% HCl solution. Results from surface techniques confirm adsorption of GA-AgNPs molecules on specimen surface. Oxides, hydroxides, carbonates, and sulphates (H2SO4 medium) or chlorides (HCl medium) are the corrosion products in the free corrodent according to XPS results. In the presence of composite, both ionic and neutral forms of GA-AgNPS are adsorbed. AgNPs are present on the surface in the form: Ag°, Ag2O, and AgO. The conclusion of a green formulation consisting of gum Arabic, silver nanoparticles, and residual natural honey has been developed. The anticorrosion property of the prepared nanocomposite has been examined using several techniques. The results of all

applied techniques show that the composite is effective in inhibiting the steel corrosion in 15% H2SO4 and 15% HCl solutions respectively. The composite molecules absorb onto the metal surface and protect the surface from further attack by aggressive agents present in the corrosive environments. The adsorption followed Langmuir adsorption isotherm model. GA-AgNPs acted as mixed type inhibitor in 15% H2SO4 solution but as anodic type inhibitor in 15% HCl solution. Inhibition is better in HCl medium. XPS results disclose that the corrosion products in the absent of composite are FeO, FeCO3, Fe2O3, and FeSO4(H2SO4 medium) or FeCl3 (HCl medium). In the presence of composite, gum arabic is present in the adsorbed film in both ionic and neutral forms while AgNPs are present in the form Ag°, Ag2O, and AgO [62].

2.9.6 Dopant profiling with the scanning electron microscope-A study of Si

S. L. Elliott, R. F. Broom do this study. This article describes a detailed study of semiconductor dopant profiling with the scanning electron microscope (SEM) using secondary elecu•ons. The technique has been applied to a wide variety of doped silicon test structures as well as a metal—oxide field-effect transistor. We have demonstrated that contrast can be detected from p-doped regions as thin as one nanometer across. Contrast can also be measured from p-type regions with doping concentrations less than 10^{16} cm-3. And have studied the variation of doping contrast with specimen temperature and with a bias applied across a p-n junction in situ in the SEM. These experiments demonstrate that doping contrast is mainly due to the built-in voltages in semiconductor devices which in local fields (patch fields) outside the specimen which influence the number of secondary electrons detected. A concise set of guidelines is provided for users of this technique, including the optimum SEM operating conditions that should be used for maximum contrast. The conclusion a detailed study of dopant contrast from a Si p-n junction and other Si süuctures has been reported in this article. cpn varies linearly with the built-in voltage. The resolution and sensitivity limits of SEM dopant profiling have been systematically studied, with extremely promising results. Doped regions as

small as one nanometer in width as well as dopant concentrations less than 10 ^{16} cm in p-type on n-type silicon have been detected. This article has provided experimental evidence linking dopant contrast to the built-in voltage at a semiconductor junction, by biasing a p-n junction and also by measuring the contrast over a range of temperatures. The results support the effect of local fields on the secondary electrons as the dopant contrast mechanism. The results for a range of temperatures show a correlation between the built-in voltage and the magnitude of the dopant contrast, in particular both the contrast (cp n) and the built-in voltage (Vbi) decrease at higher tem- Broom, peratures. These results show that when measuring dopant contrast, the temperature is an important consideration. The biasing of the p-n junction and consequent changes in the built-in voltage show an excellent correlation with changes in the dopant contrast. This result is particularly promising for the development of this technique, as quantification may be possible with further understanding of the contrast mechanism [63].

2.9.7 Classification and physicochemical characterization of mesquite gum (Prosopis spp.)

The groups that done this work was Yolanda L. López-Franco. Under environmental stress conditions, mesquite trees can excrete a proteinaceous arabinogalactan gum that is similar to gum Arabic. Given the application potential of this type of gums a classification procedure for the mesquite gum is proposed. The main physicochemical properties of the best-quality mesquite gum were determined and compared with those of gum Arabic. Additionally, the composition and molecular changes induced by purification processes were recorded. One batch (157 kg) of mesquite gum was categorized by subjective assessment into three classes (MGA, MGB and MGC) from high- to low-quality. Approximately 17.5% was classified as top-quality gum. It was found that this class of mesquite gum has lower humidity, inorganic and tannins content than the other classes, or even than the gum Arabic sample used as a reference. All of the mesquite gum classes have higher protein content and

lower intrinsic viscosity than gum Arabic. The purification processes were shown to reduce the content of lower molecular weight compounds that modify the interface properties of the gum. The results indicate that the proposed classification method can be used to select mesquite gum with physicochemical properties comparable to those of commercial gum Arabic. The conclusions was the proposed classification procedure is a simple method for the selection of mesquite gum that meets the quality requirements of the Joint FAO/WHO Expert Committee on Food Additives (JECFA) for gum Arabic intended for drugs and foods. The highest quality selected mesquite gum (MGA) has a lower tannin, insoluble solid, inorganic and humidity content than the other classes and even the gum Arabic used as a reference. Filtration and ultrafiltration procedures can reduce the tannin content and the concentration of low molecular weight species in mesquite gum. However, these processes could modify the interface properties of the high quality mesquite gum (MGA) [64].

2.9.8 Electrical conductivity behavior of Gum Arabic biopolymer-Fe_3O_4 Nano composites

This work done by D. Bhakat. In this work present reports a study on the electrical conduction properties of some composites of Gum Arabic biopolymer and magnetite nanoparticles as host and guest, respectively, synthesized in different weight percentages. The Nano composites are found to be non-extrinsic type of semiconductors with guest content dependent trap distribution of charge carriers. Conductivity of these materials increases with increasing guest content along with a concomitant decrease in the activation energy. Percolation theory has been employed for the analysis of the electrical conductivity results to explore the effect of the guest on the electrical conductivity of the host. The conclusions are the electrical conductivity of some composites of biopolymer and inorganic nanoparticles has been studied as a function of temperature and applied bias voltage. Conductivity of these materials strongly depends on sample temperature, applied bias voltage and the weight percentage of the components. The trap distribution of charge carriers

in these materials has been estimated. Increase of the guest content changes the nature of trap distribution in these Nano composites. The activation energy of these samples is directly proportional to the guest content. In the Ohmic region the calculated small values of σ_o indicates a wide range of localized states and the conduction is taking place by the hopping process in the presently studied samples, whereas in the non-Ohmic region the conduction may be controlled by quantum tunneling mechanism. Percolation concept has been applied to understand the electrical conduction in these composites. Percolation threshold and critical exponent are inversely proportional to the guest content. This indicates that φc and μ are directly proportional to each other. The conduction mechanism in these composites may be owing to the charge carrier transfer through the guest molecule aggregations distributed in the host matrix [65].

2.9.9 Determination of the Energy Gap of Gum Arabic Doped with Zinc Oxide Using the UV-VIS Technique

This work done by ELKHATEM ELMHDY ALI MOHAMED. In this work ,Zinc Oxide Nano particle (ZnO) were successfully synthesized by a sol-gel method, then the solution of the gum Arabic was also prepared and pored by the mortar method. The samples were characterized by UV-VIS spectroscopy technique. Then the wave length was plotted vrs the absorption and calculation were done to evaluate the energy gap (Eg) using the formula (a *h*n) = *C* (*h*n − *Eg*) 2 It shows that the energy gap of gum Arabic is found to be, Eg = (2.760) eV, for both samples. Which prove that it is a real semiconductor and its conductivity increases with the increasing of the dopants Zinc Oxide (ZnO). The conclusion of this work is the defrosting of citric acid on the zinc-oxide polymer led to reducing the energy gap, the polymerization of the acid with a citric acid did not affect the nature of the electronic transitions, but negatively affected the values of the energy gap, which makes this, affect in many the field of visual and electronic applications [66].

2.9.10 covalent coupling of gum Arabic onto super paramagnetic iron oxide nanoparticles for MRI cell labeling: physicochemical and in vitro characterization

This study done by Susana I. C. J. For this work Gum arabic (GA) is a hydrophilic composite polysaccharide derived from exudates of Acacia senegal and Acacia seyal trees. It is biocompatible, possesses emulsifying and stabilizing properties and has been explored as coating agent of nanomaterials for biomedical applications, namely magnetic nanoparticles (MNPs). Previous studies focused on the adsorption of GA onto MNPs produced by co-precipitation methods. In this work, MNPs produced by a thermal decomposition method, known to produce uniform particles with better crystalline properties, were used for the covalent coupling of GA through its free amine groups, which increases the stability of the coating layer. The MNPs were produced by thermal decomposition of Fe(acac)3 in organic solvent and, after ligand-exchange with meso- 2,3-dimercaptosuccinic acid (DMSA), GA coating was achieved by the establishment of a covalent bond between DMSA and GA moieties. Clusters of several magnetic cores entrapped in a shell of GA were obtained, with good colloidal stability and promising magnetic relaxation properties (r2/r1 ratio of 350). HCT116 colorectal carcinoma cell line was used for in vitro cytotoxicity evaluation and cell-labeling efficiency studies. We show that, upon administration at the respective IC50, GA coating enhances MNP cellular uptake by 19 times compared to particles bearing only DMSA moieties. Accordingly, in vitro MR images of cells incubated with increasing concentrations of GA-coated MNP present dose-dependent contrast enhancement. The obtained results suggest that the GA magnetic Nano system could be used as a MRI contrast agent for cell-labeling applications. The CONCLUSIONS and have obtained very stable dispersions of monodisperse superparamagnetic particles (pdI = 0.2) composed by several magnetic cores entrapped in a shell of GA, with hydrodynamic diameter of 344 ± 87 nm. GA was shown to contribute to high transverse and low longitudinal MR relaxivity

values (r2/r1 ratio of 350), resulting in good MRI contrast enhancement properties, observed both in phantom images of water dispersion of MNP-DMS-GA and in in vitro MRI images of HCT116 cells incubated with different concentrations of particles. By quantification of the cellular iron after incubation for 48 h with particles, and showed that GA coating on MNP-DMSA enhances MNP cellular uptake by 19 times compared to MNP-DMSA alone. Incubation for different periods revealed that the iron uptake kinetics for MNP-DMSA-GA is fast (less than 12 h) and cellular uptake is always enhanced compared to uncoated nanoparticles. After 48 h of incubation, MNP-DMSA-GA localize in the lysosomes, which suggests uptake by endocytosis, but the evaluation of the presence of asialoglycoprotein receptors in the HCT116 cell line could give new insights on the MNP-DMSA-GA cellular uptake mechanism. We also found out that the HCT116 cell line is very sensitive to MNPs, given the observed dose-dependent cell viability decrease in MTT assay at the tested iron concentrations (IC50 valuesof 55 μg/mL for MNP-DMSA and 43 μg/mL for MNP-DMSA-GA). Apoptotic response was detected by upregulation of proapoptotic genes p21 and BAX and downregulation of antiapoptotic gene BCL-2 after 3.5 h and also at 48 h of incubation with the MNP-DMSA-GA nanoparticles (but to a lesser extent in this last time point). Nonetheless, given the large hydrodynamic diameter and the good MRI contrast enhancement properties, the MNP-DMSA-GA presents potential for in vitro MRI celllabeling applications. Further modification of GA (e.g., with a fluorophore or radionuclide) would contribute to a multimodal contrast agent, allowing to follow the labeled cells by MRI and other imaging technique(s) [67].

2.9.11Preparation, characterization and electrical study of gum Arabic/ ZnO nanocomposites

This work done by PUSPENDU BARIK . Gum arabic (GA)-mediated chemical synthesis was carried out for obtaining ZnO nanoparticles (ZnONPs) (particle size of ZnO ≈ 40 nm) which, in turn, was used for preparing ZnO–biopolymer

nanocomposites. The dielectric study of this synthesized products is reported in this paper. The synthesized products were characterized by X-ray diffraction, Fourier transform infrared, and transmission electron microscopy for their structure and morphology study. The frequency dependence of dielectric constant and dielectric loss of these GA–ZnO nanocomposites were analysed in the frequency range of 100 Hz–5 kHz. In addition, the dielectric property of these nanocomposites (0–15 wt% filler concentration) was analysed with respect to frequency in the temperature range 30–80◦C. A high dielectric constant of 275 is achieved for the sample with 10 wt% of ZnO filler. The dielectric property of GA–ZnO nanocomposites is attributed to the interfacial and orientation polarization. The conclusion in this work, the variation of dielectric constant and the dielectric loss of GA/ZnO nanocomposites, combined at different mass ratios, with temperature and frequency were found to be nonlinear experimentally. A high dielectric constant was found for the sample with 10 wt% of ZnO filler. The effect of ZnO on dielectric constant value of nanocomposites was found to be more pronounced at lower frequency region. The dielectric properties of ZnO-NPs are attributed to the interfacial and orientation polarization. The synthesized composites exhibit a low dielectric loss at higher frequency region, which is preferred to reduce the energy dissipation and signal losses, particularly for high frequency applications [68].

2.9.12 Using Gum Arabic in Making Solar Cells by Thin Films Instead of Polymers

In the work done by Abdelsakhi. 3 sample of Gum solar cells were made by depositing the Gum Arabic solution on ITO a glass by Spin Coating technical, and another layer was deposited from dye on a layer of Gum Arabic .Gold was fabricated on the layers to represent the anode and ITO Cathode. A clean glass plate with a thin layer of ITO (Indium Tin Oxide) is needed. The ITO acts as the first part of the solar cell, the first electrode. However a bit of the ITO has to be removed, to avoid short-circuiting For the purpose of the present study

Arabic Gum devices were made following the generally accepted methods. The fabrication process started by preparing the Arabic Gum and the dye of interest then spin coated on indium tin oxide glass. Silver electrode was used to complete the formation of organic Arabic Gum solar cell. The formed devices were characterized by Ultra violet-visible spectroscopy. The Arabic Gum solar cell was made on ITO glass. The ITO glasses were firstly cleaned by ethanol and distilled water. 10mg of Arabic Gum was dissolved into 0.5ml of chloroform and add 0.24 mg ZnO and added drop of acetic acid glacial. Then 3mg of Rhodamine 6G dye dissolved into 0.5 of high pure chloroform was deposited on Arabic Gum .Being inserted electrical circuit containing the (voltmeter and Ammeter and a light source Lamp with the intensity radiological" and a solar cell).Cell was offered to light and fulfilled taking the results of the current and voltages were recorded the UV spectrometer in as to display absorption spectrum. Three samples were prepared. The conclusions application of conducting Arabic Gum to optoelectronic devices such as solar cell, light emitting diodes, and electrochemical sensors are of practical significance, because the Arabic Gum mixture can be easily prepared and modified by rich chemical procedures to meet optical and electronic requirements. This solar cell is cheap can be easily fabricated. It efficiency is relatively large [69].

2.9.13 The Effect of Optical Energy Gaps on the Efficiency for Dye Sensitized Solar Cells (DSSC) by using Gum Arabic Doped by CuO and (Coumarin 500, Ecrchrom Black, Rhodamin B and DDTTc) Dyes

This work done by Mubarak Dirar Abd-alla .In this work Gum Arabic based Dye Sensitized Solar Cells (DSSC) with five types of dyes (Coumarin 500, Ecrchrom Black, Rhodamin B, DDTTc and Nile blue) were fabricated on ITO glass. Microstructure and cell performance of the solar cells with (ITO/ Gum Arabic / dye /ITO+ graphite and Iodine) structures were investigated. Photovoltaic devices based on the Gum Arabic / dye hetrojunction structures provided photovoltaic properties under illumination. Absorption and energy

gap measurement of the (Coumarin 500, Ecrchrom Black, Rhodamin B, DDTTc and Nile blue) were studied by using UV-VS mini 1240 spectrophotometer and light current-voltage characteristics. The five (ITO/ Gum Arabic / dye /ITO+ graphite) solar cells were produced and characterized, which provided efficiency (η) and Energy gap 4.92 % for Eg = 1.436 eV ,1.9 % for Eg = eV ,2.01, 0.44 % for Eg = 2.641 eV and 0.37 % for Eg = 4.197 respectively. It is very interesting to note that the efficiency increases as the energy gap decreases. However for Ecrchrom Black the efficiency is high which may be related to high transparency that allows more photons to liberate electrons from gum layer. The conclusion the efficiency of solar cells formed from gum Arabic doped with copper oxide and dyes are affected by the energy gap and transparency of dyes [70].

CHAPTER THREE

MATERIALS AND METHODS

3.1 Introduction

Gum samples were collected from local marketing. The gum was dried at room temperature and kept in plastic containers for analysis.

3.2 Materials

3.2.1 Gum Arabic

Acacia gum is a natural agricultural resource from the gum belt region of Africa, i.e., countries geographically ranging from east to west: from Sudan, Somalia, Eritrea, and Ethiopia to Chad, Central African Republic, Mali, Niger, and farther west up to Nigeria, Senegal, and even Mauritania (Mohammed, 2011). Economically speaking, acacia gum mainly comes from Sudan, Chad, and Nigeria. In Sudan, the most important of nonwood forest products is gum Arabic, which exudates from Acacia senegal and locally known as hashab, or hard gum, and *Acacia seyal*, which is known as talha, or friable gum. Both species spread naturally in the central belt of the low-rainfall savannah, where they exist in pure or mixed stands, in the clay plains in the East, and the sandy soils in the West (ElKhawad, 2008). Despite the significant contribution of *A. seyal* to the exports market in the Sudan, farmers have a slightly poor knowledge of postharvest cultural practices of *A*. *seyal*, which include proper methods of storage conditions and gum stacking. Nevertheless, this chapter is trying to review the existing research in the areas of pre- and postharvest cultural practices, including tree husbandry, tapping, gum collection, handling, and storage. Physical and chemical properties of *A. seyal* establish a clear protocol of the *A. seyal* tree in the Sudan.

3.3 Method

The unlopped and Gum Arabic (Talha and Hashaba) doped by Iodine with rated (0.1, 0.3 ,0.5 ,0.7 and 0.9) m Molar were synthesized by chemical precipitation method were dissolved in100 mL double distilled water (de-ionized water) separately under stirring at room temperature**,** drop wise addition of Iodine with

rated (0.1, 0.3 ,0.5 ,0.7 and 0.9) m Molar solution was stirred using magnetic stirrer at 3000 rpm for 2 hours at room temperature. Then the annealed sample was grinded to get the powdered nanoparticles.

The crystal structure of all samples characterized at room temperature using a Philips PW1700 X-ray diffractometer (operated at 40 kV and current of 30 mA). The infrared spectra of synthesized FTIR (Fourier Transform Infrared Spectrophotometer) in the range of 400 to 4000 cm^{-1} which used to locate the band positions which are given for all samples. The optical properties of all samples characterized at room temperature using min 1240 UV- Spectroscopy. From optical spectra of synthesized calculate all optical properties (Absorption Coefficient, Extinction coefficient, Optical Energy Band Gap, Refractive Index, Real Dielectric Constant and Imaginary Dielectric Constant)

3.4 Characterization Techniques

The Materials Characterization Lab has a wide variety of characterization techniques in the areas of X-ray diffractometer, FTIR (Fourier Transform Infrared Spectrophotometer), and min 1240 UV- Spectroscopy techniques which help to increase the different degrees of understanding why different materials show different properties and behaviors.

To investigate the optical properties of Gum Arabic (Talha and Hashaba) doped by Iodine with rated (0.1, 0.3, 0.5, 0.7 and 0.9) m Molar nanoparticles, some precise techniques have been used in our stud. The following characterizations have been potentially performed for the analytical of the synthesized samples.

3.4.1Fourier transport infrared spectroscopy (FTIR)

Infrared (IR) spectroscopy is a one-photon effect and the photon absorption results in a vibrational motion of a molecule. Infrared spectra originate from the vibrational motions of atoms in chemical bonds within the molecular structure. When a beam of light containing the (IR) radiation interacts with a sample [79]. Fourier spectroscopy" is a general term that describes the analysis of any varying signal into its constituent frequency components, Fourier

Transform Infrared Spectroscopy (FTIR) is a reliable method of infrared spectroscopy and offers several analytical opportunities in academic, analytical and forensic labs, FT-IR spectroscopy includes the absorption, reflection, emission, or photoacoustic spectrum obtained by Fourier transform of an optical interferogram [80].

The infrared region (10-14000 cm-1) of the electromagnetic spectrum is divided into three regions: the near-, mid-, and far-IR. The mid-IR (400-4000 cm-1) is the most commonly used region for analysis as all molecules possess characteristic absorbance frequencies and primary molecular vibrations in this range. Mid-infrared spectroscopy

Methods are based on studying the interaction of infrared radiation with samples. As IR radiation is passed through a sample, specific wavelengths are absorbed causing the chemical bonds in the material to undergo vibrations such as stretching, contracting, and bending. Functional groups present in a molecule tend to absorb IR radiation in the same wavenumber range regardless of other structures in the molecule, and spectral peaks are derived from the absorption of bond vibrational energy changes in the IR region. Thus there is a correlation between IR band positions and chemical structures in the molecule. In addition to providing qualitative information about functional groups, IR spectra can provide quantitative information, such as the concentration of bacteria in a growth medium. An IR spectrum is measured by calculating the intensity of the IR radiation before and after it passes through aSample and the spectrum is traditionally plotted with Y-axis units as absorbance or transmittance and the X- axis as wave number units.For quantitative purposes it is necessary to plot the spectrum in absorbance units [81].

FT-IR absorbance spectra follow Beer‘s law, which relates concentration to absorbance as in Eq. (3.1)

$$A_\lambda = L\, \varepsilon_\lambda C \qquad (3.1)$$

Where A_λ_= Absorbance, L = Path length, ε_λ = Absorptivity, c = Concentration

Transmittance is not directly proportional to the concentration and is defined in Eq. (3.2)

$$\%T = \frac{I_S}{I_R} \qquad (3.2)$$

Where I_S = Intensity of IR beam after passing through the sample, I_R = Intensity of IR beam before passing through the sample, T= Transmittance Fourier transport infrared (FTIR) spectra of samples were detected by (Mattson,

Model 960m0016) spectra with transmission from 4000 to 400cm^{-1}, by using KBr pellets seen fig (3.1).

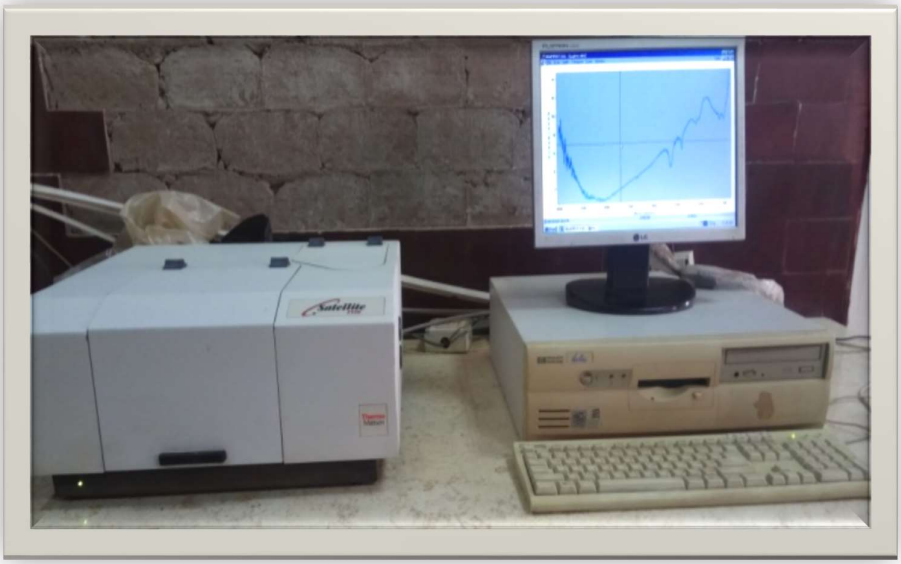

Figure (3.1): FTIR (Mattson, model 960m0016) spectroscopy.

3.4.2 Ultraviolet -visible spectroscopy (UV-Vis)

Ultraviolet and Visible Spectroscopy is absorption spectroscopy uses electromagnetic radiations between 190 nm to 800 nm and is divided into the ultraviolet (UV, 190-400 nm) and visible (VIS, 400-800 nm) regions. Since the absorption of ultraviolet or visible radiation by a molecule leads transition among electronic energy levels of the molecule, it is also often called as electronic spectroscopy [82].When radiation interacts with matter, a number of processes can occur, including reflection, scattering, absorbance,

Fluorescence/phosphorescence (absorption and reemission), and photochemical reaction (absorbance and bond breaking). In general, when measuring UV-visible spectra, we want only absorbance to occur. Because light is a form of energy, absorption of light by matter causes the energy content of the molecules (or atoms) to increase. The total potential energy of a molecule generally is represented as the sum of its electronic, vibrational, and rotational energies [83, 84].

The absorption spectra of prepared nanoparticles were measured using shimadzu spectrophotometer (UV mini 1240) in 190-800nm range see Fig (3.2)

Figure (3.2): UV mini 1240 spectrometer shimadzu

3.4.3 X-ray Powder Diffraction (XRD)

X-ray diffractometers consist of three basic elements: an X-ray tube, a sample holder, and an X-ray detector. X-rays are generated in a cathode ray tube by heating a filament to produce electrons, accelerating the electrons toward a target by applying a voltage, and bombarding the target material with electrons. When electrons have sufficient energy to dislodge inner shell electrons of the target material, characteristic X-ray spectra are produced. These spectra consist

of several components, the most common being Kα and Kβ. Kα consists, in part, of Kα1 and Kα2. Kα1 has a slightly shorter wavelength and twice the intensity as Kα2. The specific wavelengths are characteristic of the target material (Cu, Fe, Mo, and Cr). Filtering, by foils or crystal monochrometers, is required to produce monochromatic X-rays needed .for diffraction. Kα1and Kα2 are sufficiently close in wavelength such that a weighted average of the two is used. Copper is the most common target material for single-crystal diffraction, with CuKα radiation = 1.5418Å. These X-rays are collimated and directed onto the sample. As the sample and detector are rotated, the intensity of the reflected X-rays is recorded. When the geometry of the incident X-rays impinging the sample satisfies the Bragg Equation, constructive interference occurs and a peak in intensity occurs. A detector records and processes this X-ray signal and converts the signal to a count rate which is then output to a device such as a printer or computer monitor. The geometry of an X-ray diffractometer is such that the sample rotates in the path of the collimated X-ray beam at an angle θ while the X-ray detector is mounted on an arm to collect the diffracted X-rays and rotates at an angle of 2θ. The instrument used to maintain the angle and rotate the sample is termed a goniometer. For typical powder patterns, data is collected at 2θ from ~5° to 70°, angles that are preset in the X-ray scan. [1]

Figure (3.3) X-Ray diffract meter: XRD (wavelength 1.54 A°)

CHAPTER FOUR

RESULTS AND DISCUSSION

4.1 Introduction

In this part of research, the main results that have been obtained from the experiments made of (Talha Gum Arabic+ Iodine) (0.1, 0.3, 0.5, 0.7 and 0.9) m Molar and (Hashaba Gum Arabic+ Iodine) (0.1, 0.3, 0.5, 0.7 and 0.9) m Molar where Nanomaterials are presented. The data of X-ray diffraction (XRD) have been analyzed by using Rietveld method to ensure good quality of the samples (their crystal structure, their lattice parameters, the positions of atoms within the cell), the FT-IR data have been carried to investigate the chemical bonds within atoms and the data of UV-visible used to evaluate the band gap

4.2 Optical Results of (Talha Gum Arabic + Iodine) samples

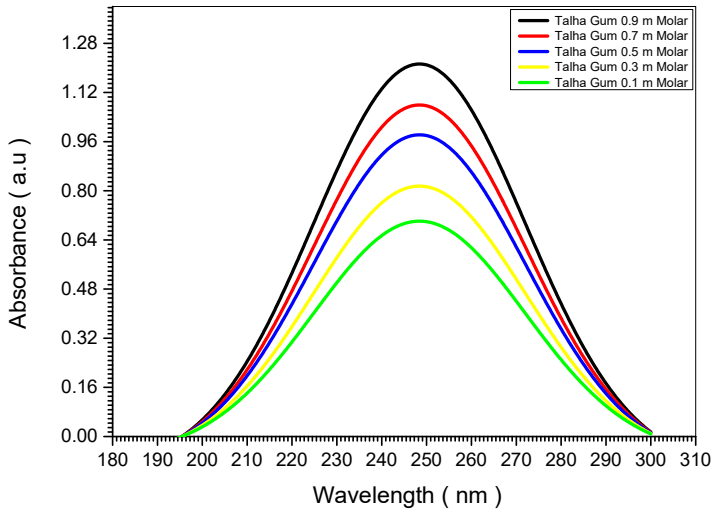

Figure(4.1) The relation between absorbance and wavelengths of five Talha Gum Arabic + Iodine samples (0.1, 0.3, 0.5, 0.7 and 0.9) m Molar

The absorbance we found the behavior of curves is the same for five samples of Talha Gum Arabic doping by Iodine (0.1, 0.3, 0.5, 0.7 and 0.9) m Molar studied using UV-VS min 1240 spectrophotometer. Show all resolute of

absorbance in fig (4.1). In fig. (4.1) shows the relation between absorbance and wavelengths for five samples of Talha Gum Arabic doping by Iodine (0.1 ,0.3 ,0.5 ,0.7 and 0.9) m Molar, the rapid increase of the a absorption at wavelengths 250 nm crosponding photon energy 4.96 eV by doping increase.

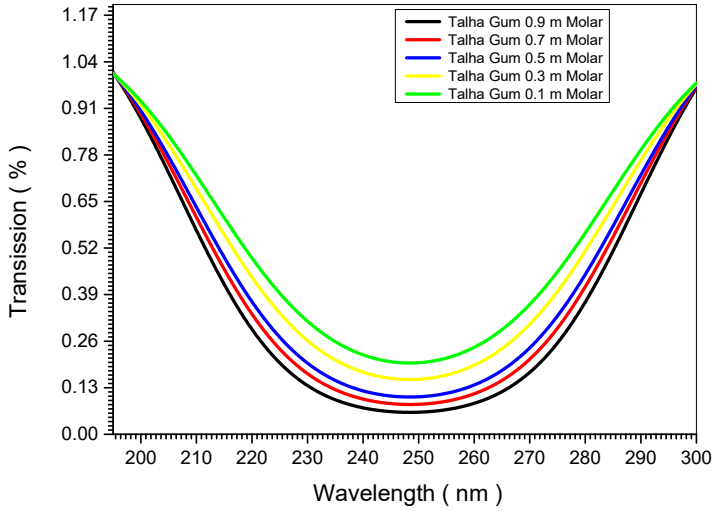

Figure(4.2) relation between transission and wavelengths of five Talha Gum Arabic + Iodine samples (0.1, 0.3, 0.5, 0.7 and 0.9) m Molar

The transission we found the behavior of curves is the same for five samples of Talha Gum Arabic doping by Iodine (0.1, 0.3, 0.5, 0.7 and 0.9) m Molar that showing in fig (4.2). In fig. (4.2) shows the relation between transission and wavelengths for five samples of Talha Gum Arabic doping by Iodine, the efficet of doping on the transission was increase doping decrease transission .

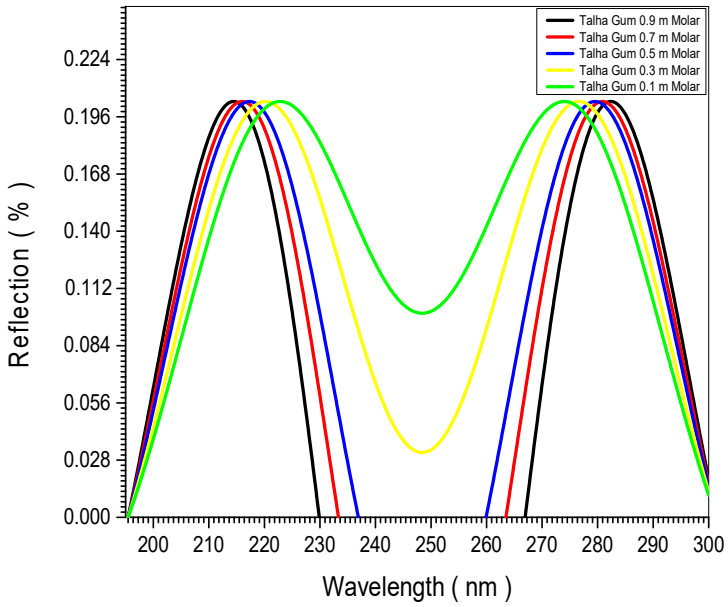

Figure(4.3) relation between reflection and wavelengths of five Talha Gum Arabic + Iodine samples (0.1, 0.3, 0.5, 0.7 and 0.9) m Molar

The reflection with five samples of Talha Gum Arabic doping by Iodine (0.1, 0.3, 0.5, 0.7 and 0.9) m Molar that showing in fig (4.3). In fig. (4.3) shows that the reflection for five samples of Talha Gum Arabic doping by Iodine was maximal value in tow area the first one in ranged (213 to 223) nm the second (273 to 283) nm in this tow point the samples become mirrors. The efficet of doping on the refelection was increase doping the transission in red sheft in first point and plue sheft in the second point .

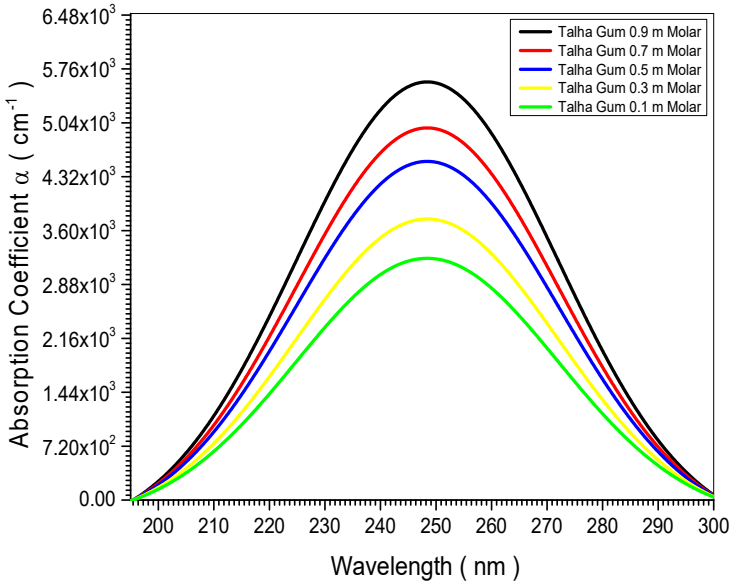

Figure(4.4) relation between absorption coefficient and wavelengths of five Talha Gum Arabic + Iodine samples (0.1, 0.3, 0.5, 0.7 and 0.9) m Molar

The absorption coefficient (α) of the five prepared sample by Talha Gum Arabic doing by Iodine (0.1 ,0.3 ,0.5 ,0.7 and 0.9) m Molar samples were found from the following relation $\alpha = \frac{2.303xA}{t}$ where (A) is the absorbance and (t) is the optical legth in the samples . In fig (4.4) shows the plot of (α) with wavelength (λ) of five sample was tretednent by Talha Gum Arabic + Iodine samples (0.1 ,0.3 ,0.5 ,0.7 and 0.9) m Molar , which obtained that the value of $\alpha = 5.59x10^3$ cm^{-1} for Talha Gum 0.9 m Molar sample in the U.V region(250 nm) but for Talha Gum 0.1 m Molar sample equal $3.22x10^3$ cm^{-1} at the same wavelength , this means that the transition must corresponding to a direct electronic transition, and the properties of this state are important since they are responsible for electrical conduction. Also, fig.(4.4) shows that the value of (α) for the five samples of Talha Gum Arabic doing by Iodine (0.1 ,0.3 ,0.5 ,0.7 and 0.9) m Molar samples increase while doing increased .

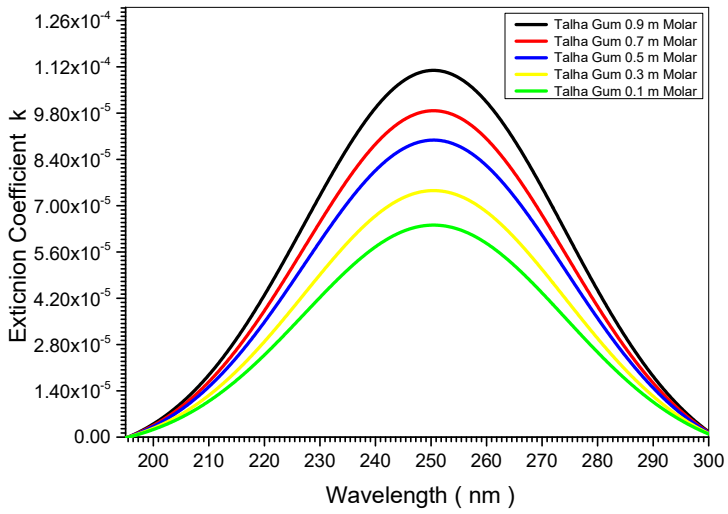

Figure(4.5) relation between exticion coefficient and wavelengths of five Talha Gum Arabic + Iodine samples (0.1, 0.3, 0.5, 0.7 and 0.9) m Molar

Extinction coefficient (K) was calculated using the related $k = \frac{\alpha\lambda}{4\pi}$ The variation at the (K) values as a function of (λ) are shown in fig. (4.5) for fivet samples of Talha Gum Arabic doing by Iodine (0.1 ,0.3 ,0.5 ,0.7 and 0.9) m Molar samples and it is observed that the spectrum shape of (K) as the same shape of (α). The Extinction coefficient (K) for five samples of Talha Gum Arabic doing by Iodine (0.1 ,0.3 ,0.5 ,0.7 and 0.9) m Molar samples in fig.(4.5) obtained the value of (K) at the (250 nm) wavelength was depend on the samples treatment method , where the value of (K) at 250 nm for Talha Gum 0.9 mMolar sample equal $1.12x10^{-5}$ while for other sample Talha Gum 0.1 mMolar at the some wavelength equal $6.39x10^{-5}$ .The effects of Iodine doping on Talha Gum Arabic doing by Iodine (0.1 ,0.3 ,0.5 ,0.7 and 0.9) m Molar samples was increased the iodine doping increased Extinction coefficient (k).

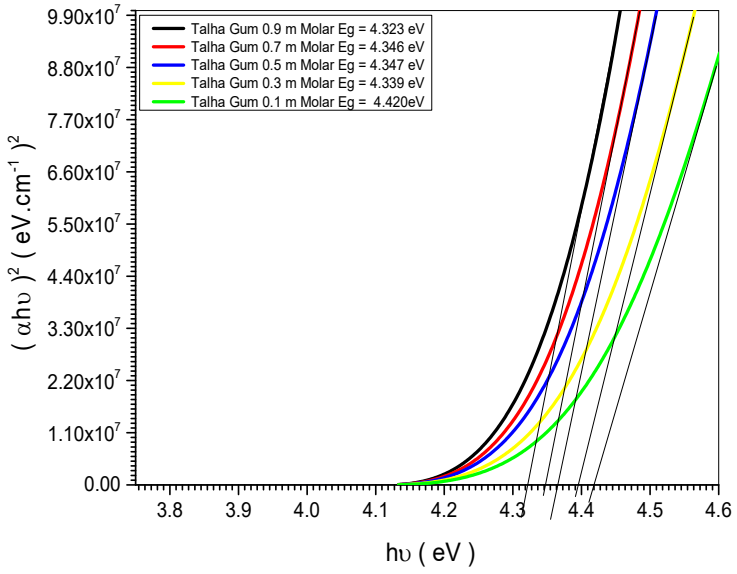

Figure(4.6) optical energy band gap of five Talha Gum Arabic + Iodine samples (0.1, 0.3, 0.5, 0.7 and 0.9) m Molar

The optical energy gap (Eg) has been calculated by the relation $(\alpha h\upsilon)^2 = C(h\upsilon - Eg)$ where (C) is constant. By plotting (αhυ)2 vs photon energy (hυ) as shown in fig.(4.6) for the five prepared by Talha Gum Arabic doing by Iodine (0.1 ,0.3 ,0.5 ,0.7 and 0.9) m Molar samples . And by extrapolating the straight thin portion of the curve to intercept the energy axis , the value of the energy gap has been calculated .In fig (4.6) the value of (Eg) Talha Gum Arabic doing by Iodine 0.9 m Molar sample obtained was (4.323) eV while for other sample Talha Gum Arabic doing by Iodine 0.1 m Molar sample obtained was (4.420) eV.The value of(Eg) was decreased from (4.420) eV to (4.323) eV. The decreasing of (Eg) related to increased of Iodine molar on the samples. It was observed that the different Iodine molar for Talha Gum Arabic doing by Iodine (0.1 ,0.3 ,0.5 ,0.7 and 0.9) m Molar samples confirmed the reason for the band gap shifts .

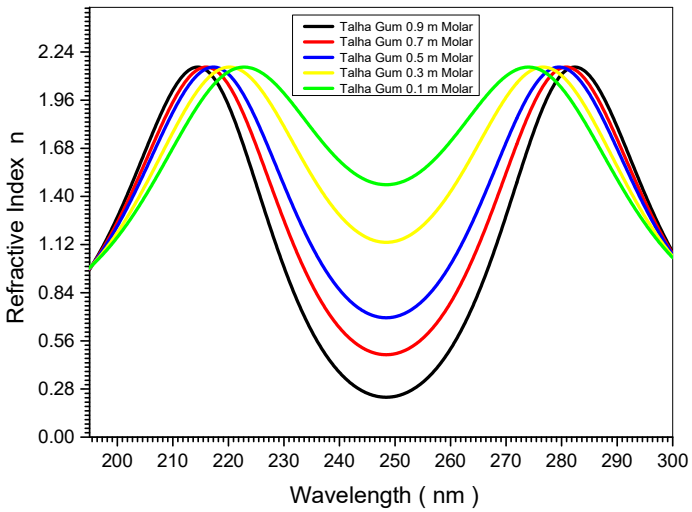

Figure(4.7) relation between refractive index and wavelengths of five Talha Gum Arabic + Iodine samples (0.1, 0.3, 0.5, 0.7 and 0.9) m Molar

The refractive index (n) is the relative between speed of light in vacuum to its speed in material which does not absorb this light. The value of n was calculated from the equation $n = [\left(\frac{(1+R)}{(1-R)}\right)^2 - (1 + k^2)]^{\frac{1}{2}} + \frac{(1+R)}{(1-R)}$ Where (R) is the reflectivity. The variation of (n) vs (λ) for five samples was treetetment by Talha Gum Arabic doing by Iodine (0.1 ,0.3 ,0.5 ,0.7 and 0.9) m Molar samples is shown in fig.(4.7). Fig (4.7) Show that relationsheep of five prepared sample by Talha Gum Arabic doing by Iodine (0.1 ,0.3 ,0.5 ,0.7 and 0.9) m Molar samples refractive index (n) spectra,which shows that the maximum value of (n) is (2.158) for all samples at tow area the first one in ranged (213 to 223) nm the second (273 to 283) nm, the point was agreement with red sheft on the first point and plue shefte on the second point by increase for Iodine doping . Also we can show that the value of (n) begin to decrease befor 213 nm and after 283 nm of region spectrum .

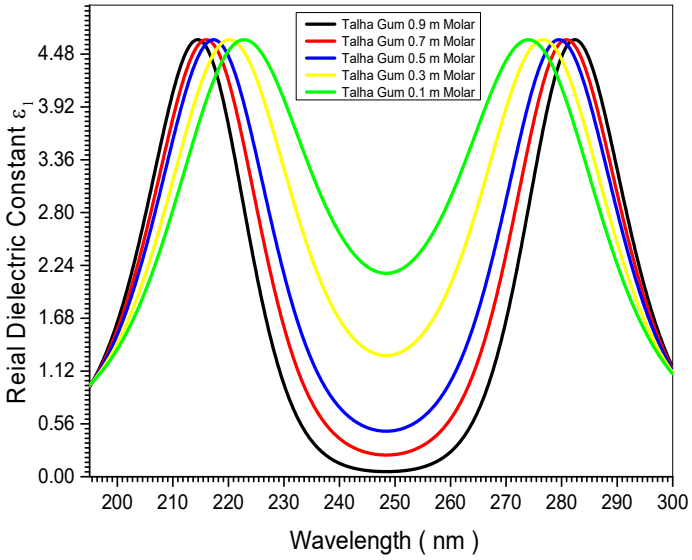

Figure(4.8) relation between real dielctric constant and wavelengths of five Talha Gum Arabic + Iodine samples (0.1, 0.3, 0.5, 0.7 and 0.9) m Molar

Real Dielectric Constant (ε_1) in Fig(4.8) shows the variation of the realdielectric constant (ε_1) with wavelengthof five samples prepared by Talha Gum Arabic doing by Iodine (0.1 ,0.3 ,0.5 ,0.7 and 0.9) m Molar samples form, which calculatedfrom the relation $\varepsilon_1 = n^2 - k^2$ Where the real the dielectric (ε_1) is the normal dielectric constant . From fig (4.8) the variation of (ε_1) is follow the refractive index, where at tow area the first one in ranged (213 to 223) nm the second (273 to 283) nm for all samples of Talha Gum Arabic doing by Iodine (0.1 ,0.3 ,0.5 ,0.7 and 0.9) m Molar samples, where theabsorption of the samples at these wavelength is small, but the polarizationwas increase. The maximum value of (ε1) equal to (4.64) at at tow area the first one in ranged (213 to 223) nm the second (273 to 283) nm. The effect of treetetment by Iodine (0.1 ,0.3 ,0.5 ,0.7 and 0.9) m Molar on the (ε1) was red sheft on the first point and plue shefte on the second point by increase for Iodine doping .

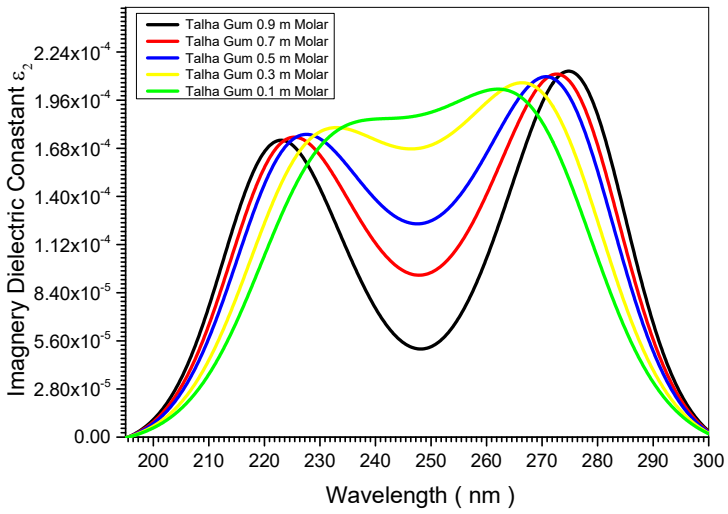

Figure(4.9) relation between imagnery dielctric constant and wavelengths of five Talha Gum Arabic + Iodine samples (0.1, 0.3, 0.5, 0.7 and 0.9) m Molar.

The imaginary dielectric constant (ε_2) vs (λ) was shown in fig(4.7) this valuecalculated from the relation $\varepsilon_2 = 2nK$ (ε_2) represent the absorption associated with free carriers.Asshown in fig(4.9) the shape of (ε_2)is the same as (ε_1), this means that the refractive index was dominated in these behavior . The maximum values of (ε_2) are different according to the tratment operation , so the maximum value of (ε1) equal to (4.64) at at tow area the first one in ranged (213 to 223) nm the second (273 to 283) nm Talha Gum Arabic doing by Iodine (0.1 ,0.3 ,0.5 ,0.7 and 0.9) m Molar samples but (ε_2) for this sample equal ($1.78x10^{-4}$) for first point and ($2.14x10^{-4}$) for the second point,these behavior may by related to the different absorption mechanism forfree carriers.

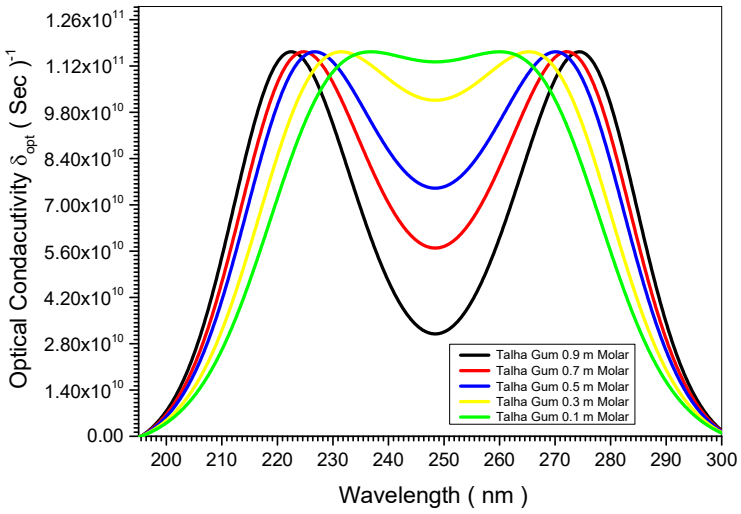

Figure(4.10) relation between optical conductivity and wavelengths of five Talha Gum Arabic + Iodine samples (0.1, 0.3, 0.5, 0.7 and 0.9) m Molar.

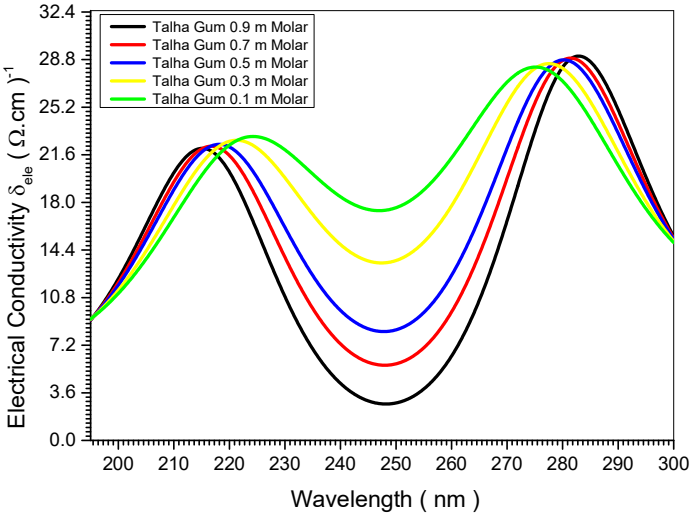

Figure(4.11) relation between electrical conductivity and wavelengths of five Talha Gum Arabic + Iodine samples (0.1, 0.3, 0.5, 0.7 and 0.9) m Molar.

Electrical and the optical conductivity is a measure of frequency response of material when irradiated with light which is determined using the following relation, $\delta_{opt} = \frac{\alpha nc}{4\pi}$ Where (c) is the light velocity. The electrical conductivity can be estimated using the following relation $\delta_{ele} = \frac{2\lambda\delta_{opt}}{\alpha}$. The high

magnitude of optical conductivity ($1.166x10^{11}$ sec^{-1}) confirms the presence of very high photo-response of the five samples prepared by Talha Gum Arabic doing by Iodine (0.1 ,0.3 ,0.5 ,0.7 and 0.9) m Molar samples . The increased of optical conductivity at high photonenergies is due to the high absorbance of five samples prepared by Talha Gum Arabic doing by Iodine (0.1 ,0.3 ,0.5 ,0.7 and 0.9) m Molar samples formand may be due to electron excitation by photon energy as it is shown in Figs (4.10) and (4.11) .

4.3 Optical Results of (Hashaba Gum Arabic + Iodine) samples

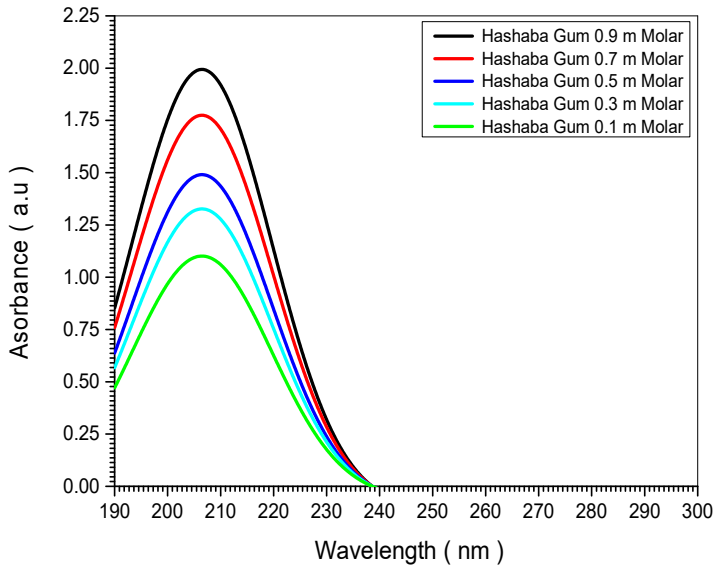

Figure(4.12) The relation between absorbance and wavelengths of five Hashaba Gum Arabic + Iodine samples (0.1, 0.3, 0.5, 0.7 and 0.9) m Molar.

The absorbance of five samples meade frome Hashaba Gum Arabic doping by Iodine (0.1, 0.3, 0.5, 0.7 and 0.9) m Molar was showing in fig (4.12). In fig. (4.12) shows the relation between absorbance and wavelengths for five samples of Hashaba Gum Arabic doping by Iodine (0.1 ,0.3 ,0.5 ,0.7 and 0.9) m Molar, the rapid increase of the a absorption at wavelengths 205 nm crosponding photon energy 6.049 eV by doping increase.

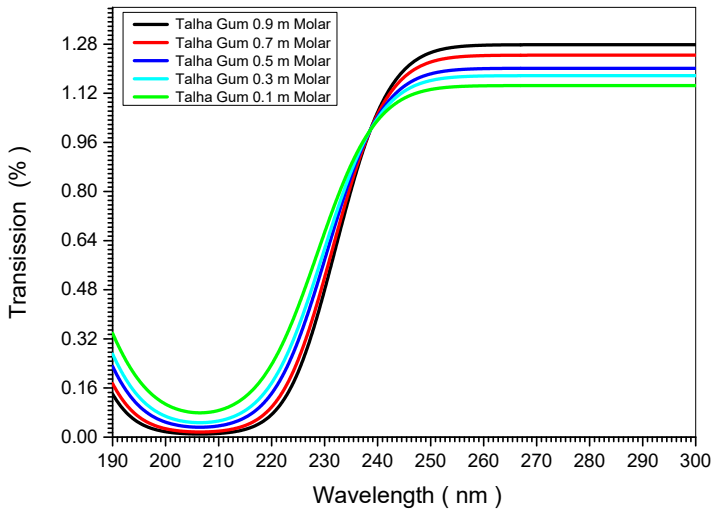

Figure(4.13) relation between transission and wavelengths of five Hashaba Gum Arabic + Iodine samples (0.1, 0.3, 0.5, 0.7 and 0.9) m Molar

The transission found the behavior of curves is the same for five samples of Hashaba Gum Arabic doping by Iodine (0.1, 0.3, 0.5, 0.7 and 0.9) m Molar that showing in fig (4.13). In fig. (4.13) shows the relation between transission and wavelengths for five samples of Hashaba Gum Arabic doping by Iodine, the efficet of doping on the transission was increase doping decrease transission .

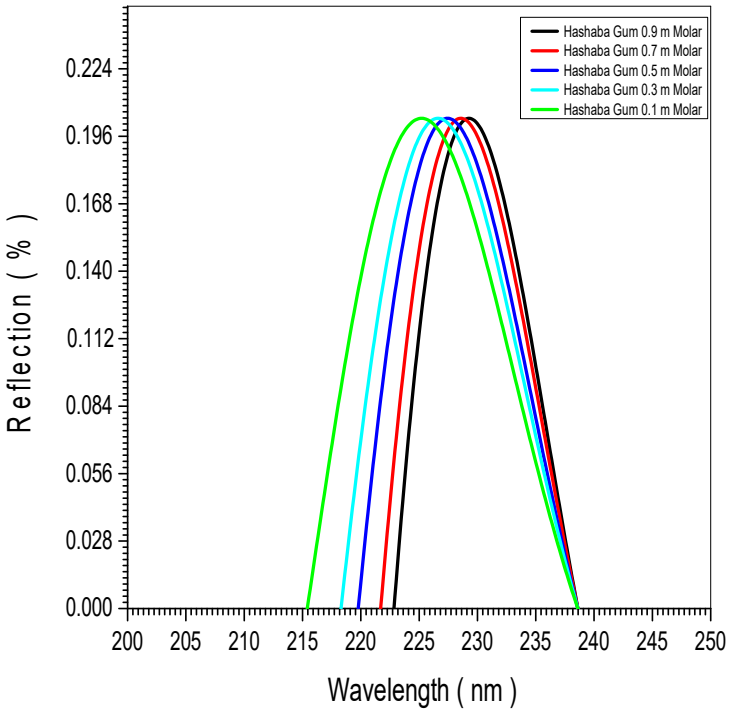

Figure(4.14) relation between reflection and wavelengths of five Hashaba Gum Arabic + Iodine samples (0.1, 0.3, 0.5, 0.7 and 0.9) m Molar

The reflection with five samples of Hashaba Gum Arabic doping by Iodine (0.1, 0.3, 0.5, 0.7 and 0.9) m Molar that showing in fig (4.14). In fig. (4.14) shows that the reflection for five samples of Hashaba Gum Arabic doping by Iodine was maximal value at wavelength ranged (225to 230) nm. The efficet of doping on the refelection was increase doping the transission was red sheft for the maximumal value of transission .

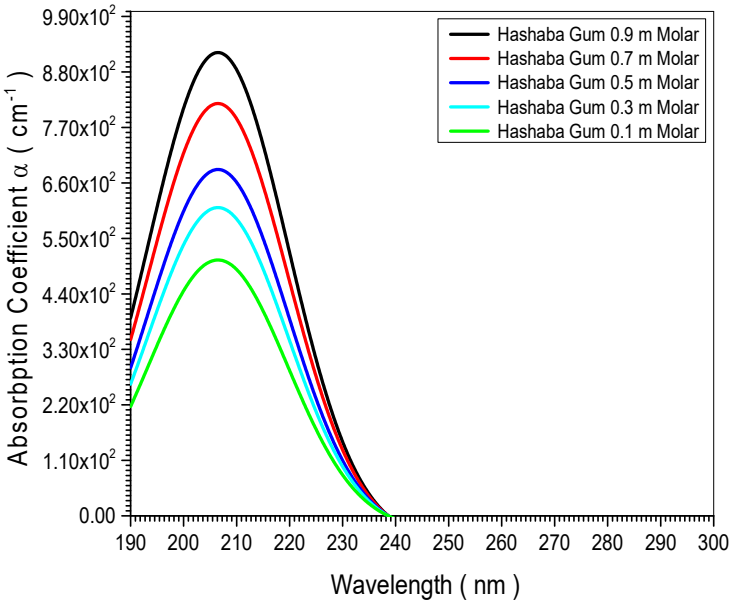

Figure(4.15) relation between absorption coefficient and wavelengths of five Hashaba Gum Arabic + Iodine samples (0.1, 0.3, 0.5, 0.7 and 0.9) m Molar

The absorption coefficient (α) of the five prepared sample by Hashaba Gum Arabic doing by Iodine (0.1 ,0.3 ,0.5 ,0.7 and 0.9) m Molar samples were found from the following relation $\alpha = \frac{2.303xA}{t}$ where (A) is the absorbance and (t) is the optical legth in the samples . In fig (4.15) shows the plot of (α) with wavelength (λ) of five sample was tretednent by Hashaba Gum Arabic + Iodine samples (0.1 ,0.3 ,0.5 ,0.7 and 0.9) m Molar , which obtained that the value of $\alpha = 9.2x10^2$ cm^{-1} for Hashaba Gum 0.9 m Molar sample in the U.V region(205 nm) but for Hashaba Gum 0.1 m Molar sample equal $5.1x10^2$ cm^{-1} at the same wavelength , this means that the transition must corresponding to a direct electronic transition, and the properties of this state are important since they are responsible for electrical conduction. Also, fig.(4.15) shows that the value of (α) for the five samples of Hashaba Gum Arabic doing by Iodine (0.1 ,0.3 ,0.5 ,0.7 and 0.9) m Molar samples increase while doing increased .

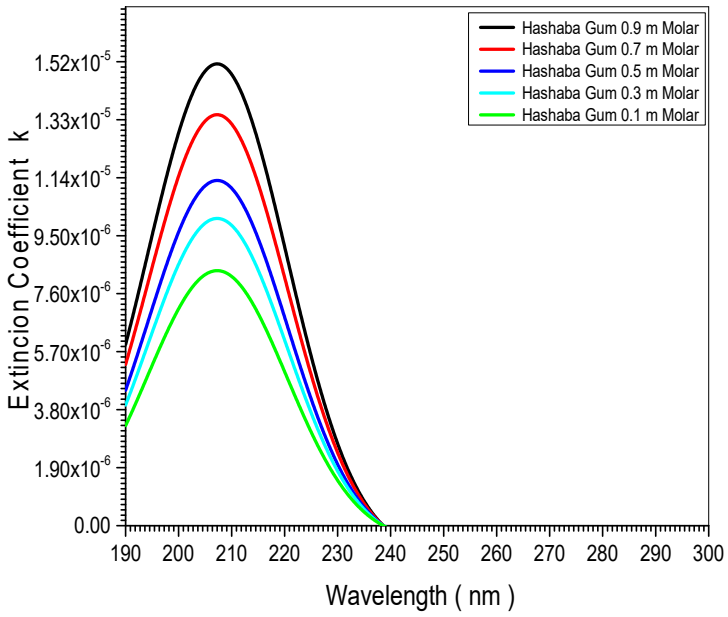

Figure(4.16) relation between exticion coefficient and wavelengths of five Hashaba Gum Arabic + Iodine samples (0.1, 0.3, 0.5, 0.7 and 0.9) m Molar

Extinction coefficient (K) was calculated using the related $k = \frac{\alpha\lambda}{4\pi}$ The variation at the (K) values as a function of (λ) are shown in fig. (4.16) for fivet samples of Hashaba Gum Arabic doing by Iodine (0.1 ,0.3 ,0.5 ,0.7 and 0.9) m Molar samples and it is observed that the spectrum shape of (K) as the same shape of (α). The Extinction coefficient (K) for five samples of Hashaba Gum Arabic doing by Iodine (0.1 ,0.3 ,0.5 ,0.7 and 0.9) m Molar samples in fig.(4.16) obtained the value of (K) at the (205 nm) wavelength was depend on the samples treatment method , where the value of (K) at 250 nm for Hashaba Gum 0.9 mMolar sample equal $1.52x10^{-5}$ while for other sample Hashaba Gum 0.1 mMolar at the some wavelength equal $8.3x10^{-6}$ .The effects of Iodine doping on Hashaba Gum Arabic doing by Iodine (0.1 ,0.3 ,0.5 ,0.7 and 0.9) m Molar samples was increased the iodine doping increased Extinction coefficient (k) value .

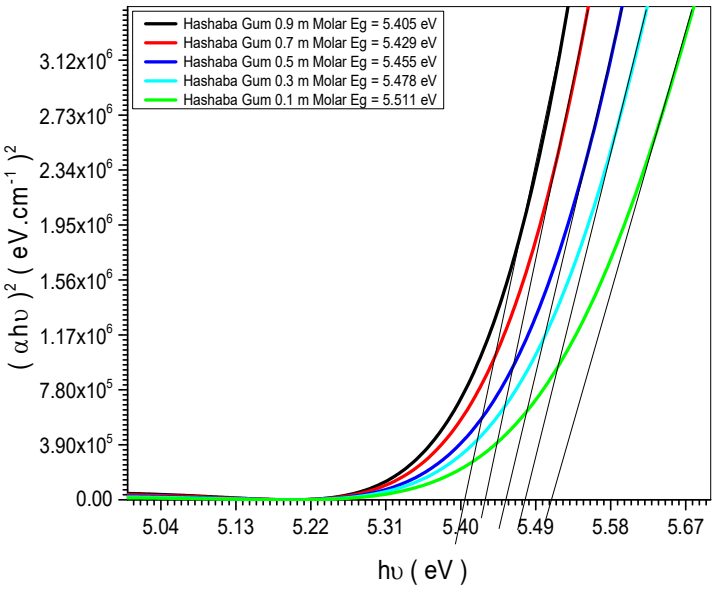

Figure(4.17) optical energy band gap of five Hashaba Gum Arabic + Iodine samples (0.1, 0.3, 0.5, 0.7 and 0.9) m Molar

The optical energy gap (Eg) has been calculated by the relation $(\alpha h\upsilon)^2 = C(h\upsilon - Eg)$ where (C) is constant. By plotting $(\alpha h\upsilon)^2$ vs photon energy ($h\upsilon$) as shown in fig.(4.17) for the five prepared by Hashaba Gum Arabic doing by Iodine (0.1 ,0.3 ,0.5 ,0.7 and 0.9) m Molar samples . And by extrapolating the straight thin portion of the curve to intercept the energy axis , the value of the energy gap has been calculated .In fig (4.17) the value of (Eg) Hashaba Gum Arabic doing by Iodine 0.9 m Molar sample obtained was (5.405) eV while for other sample Talha Gum Arabic doing by Iodine 0.1 m Molar sample obtained was (5.511) eV.The value of(Eg) was decreased from (5.511) eV to (5.405) eV. The decreasing of (Eg) related to increased of Iodine molar on the samples. It was observed that the different Iodine molar for Hashaba Gum Arabic doing by Iodine (0.1 ,0.3 ,0.5 ,0.7 and 0.9) m Molar samples confirmed the reason for the band gap shifts .

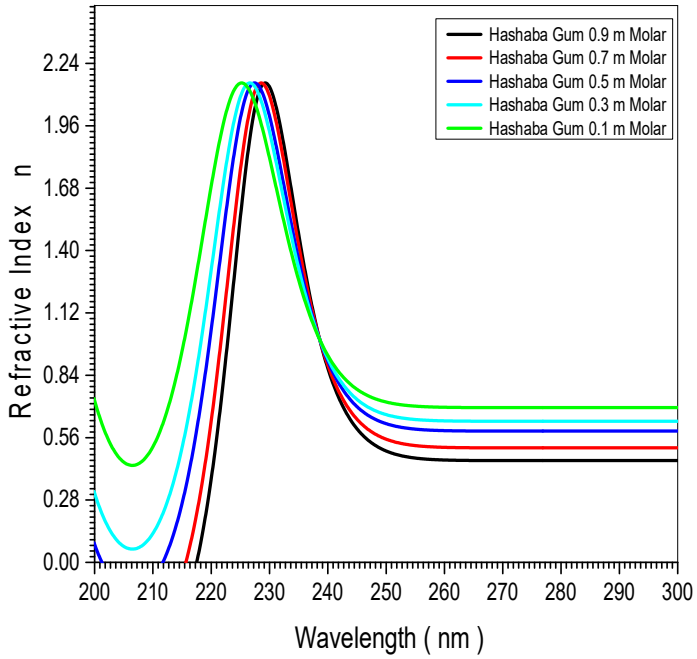

Figure(4.18) relation between refractive index and wavelengths of five Talha Gum Arabic + Iodine samples (0.1, 0.3, 0.5, 0.7 and 0.9) m Molar

The refractive index (n) is the relative between speed of light in vacuum to its speed in material which does not absorb this light. The value of n was calculated from the equation $n = [\left(\frac{(1+R)}{(1-R)}\right)^2 - (1 + k^2)]^{\frac{1}{2}} + \frac{(1+R)}{(1-R)}$ Where (R) is the reflectivity. The variation of (n) vs (λ) for five samples was treetetment by Hashaba Gum Arabic doing by Iodine (0.1 ,0.3 ,0.5 ,0.7 and 0.9) m Molar samples is shown in fig.(4.18). Fig (4.18) Show that relationsheep of five prepared sample by Hashaba Gum Arabic doing by Iodine (0.1 ,0.3 ,0.5 ,0.7 and 0.9) m Molar samples refractive index (n) spectra,which shows that the maximum value of (n) is (2.164) for all samples at wavelength ranged (224 to 230) nm, the point was agreement with red sheft by increase for Iodine doping . Also we can show that the value of (n) begin to decrease befor 230 nm on the spectrum .

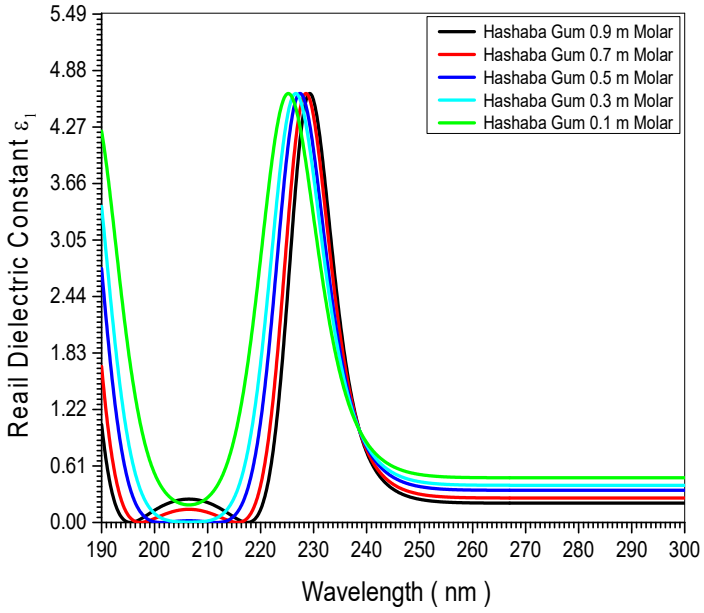

Figure(4.19) relation between real dielctric constant and wavelengths of five Talha Gum Arabic + Iodine samples (0.1, 0.3, 0.5, 0.7 and 0.9) m Molar

Real Dielectric Constant (ε_1) in Fig(4.19) shows the variation of the real dielectric constant (ε_1) with wavelengthof five samples prepared by Hashaba Gum Arabic doing by Iodine (0.1 ,0.3 ,0.5 ,0.7 and 0.9) m Molar samples form, which calculatedfrom the relation $\varepsilon_1 = n^2 - k^2$ Where the real the dielectric (ε_1) is the normal dielectric constant . From fig (4.19) the variation of (ε_1) is follow the refractive index, where at wavelength ranged (224 to 230) nm for all samples of Hashaba Gum Arabic doing by Iodine (0.1 ,0.3 ,0.5 ,0.7 and 0.9) m Molar samples, where the absorption of the samples at these wavelength is small, but the polarization was increase. The maximum value of (ε1) equal to (4.63) at wavelength ranged (224 to 230) nm. The effect of treetetment by Iodine (0.1 ,0.3 ,0.5 ,0.7 and 0.9) m Molar on the (ε1) was red sheft by increase for Iodine doping .

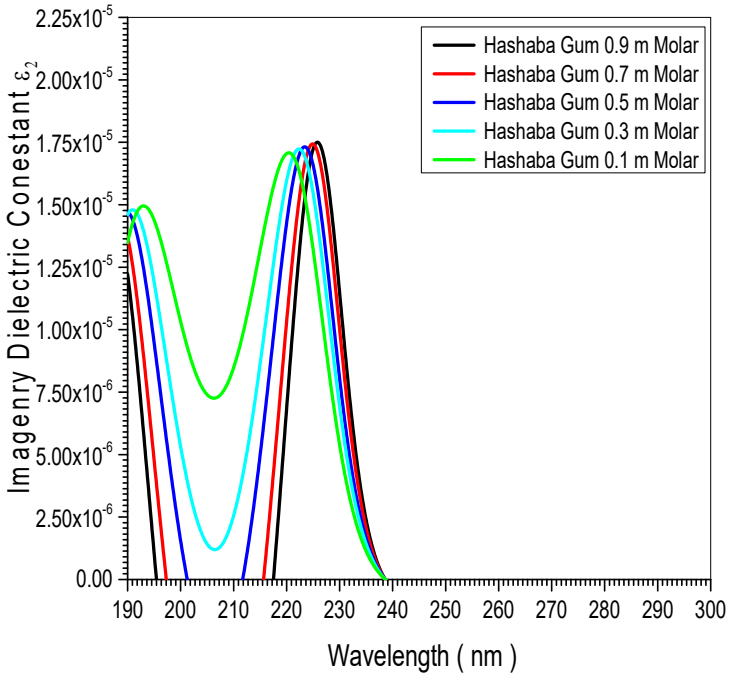

Figure(4.20) relation between imagnery dielctric constant and wavelengths of five Hashaba Gum Arabic + Iodine samples (0.1, 0.3, 0.5, 0.7 and 0.9) m Molar

The imaginary dielectric constant (ε_2) vs (λ) was shown in fig(4.20) this valuecalculated from the relation $\varepsilon_2 = 2nK$ (ε_2) represent the absorption associated with free carriers.Asshown in fig(4.20) the shape of (ε_2)is the same as (ε_1), this means that the refractive index was dominated in these behavior . The maximum values of (ε_2) are different according to the tratment operation , so The maximum value of (ε1) equal to (4.63) at wavelength ranged (224 to 230) nm, but (ε_2) for this sample equal ($1.75x10^{-5}$) ,these behavior may by related to the different absorption mechanism forfree carriers.

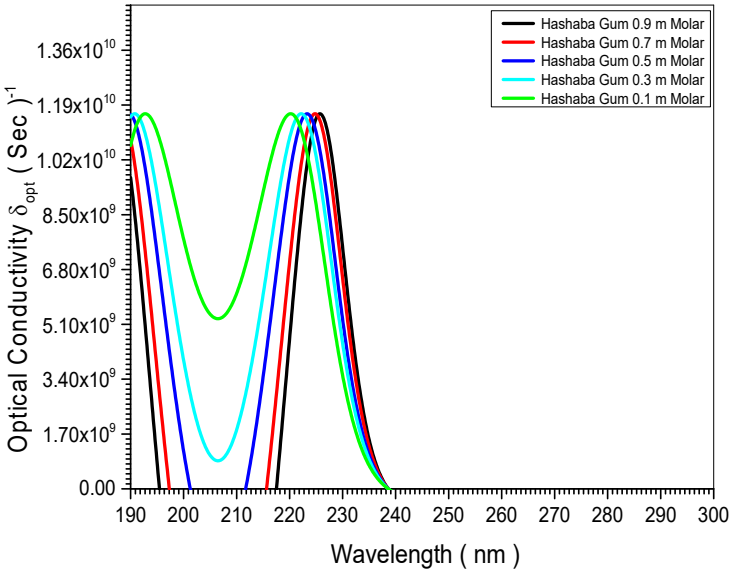

Figure(4.21) relation between optical conductivity and wavelengths of five Hashaba Gum Arabic + Iodine samples (0.1, 0.3, 0.5, 0.7 and 0.9) m Molar

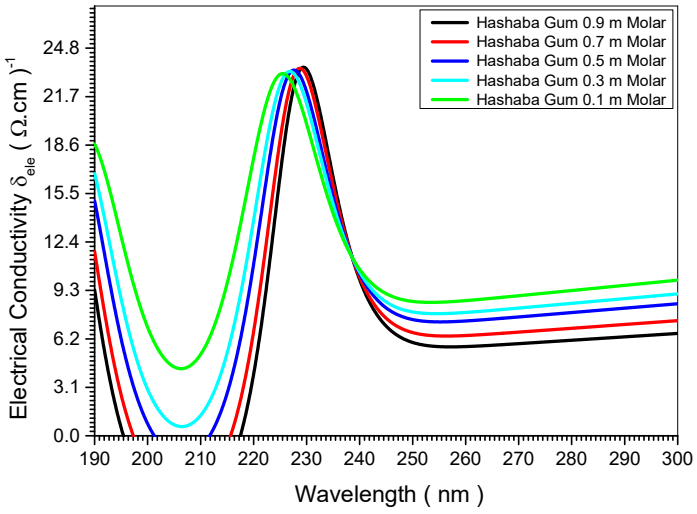

Figure(4.22) relation between electrical conductivity and wavelengths of five Hashaba Gum Arabic + Iodine samples (0.1, 0.3, 0.5, 0.7 and 0.9) m Molar

Electrical and the optical conductivity is a measure of frequency response of material when irradiated with light which is determined using the following relation, $\delta_{opt} = \frac{\alpha nc}{4\pi}$ Where (c) is the light velocity. The electrical conductivity

can be estimated using the following relation $\delta_{ele} = \frac{2\lambda\delta_{opt}}{\alpha}$. The high magnitude of optical conductivity ($1.165x10^{10}$ sec^{-1}) confirms the presence of very high photo-response of the five samples prepared by Hashaba Gum Arabic doing by Iodine (0.1 ,0.3 ,0.5 ,0.7 and 0.9) m Molar . The increased of optical conductivity at high photonenergies is due to the high absorbance of five samples prepared by Hashaba Gum Arabic doing by Iodine (0.1 ,0.3 ,0.5 ,0.7 and 0.9) m Molar form and may be due to electron excitation by photon energy as it is shown in Figs (4.21) and (4.22) .

4.4 XRD Results of (Talha Gum Arabic + Iodine) samples

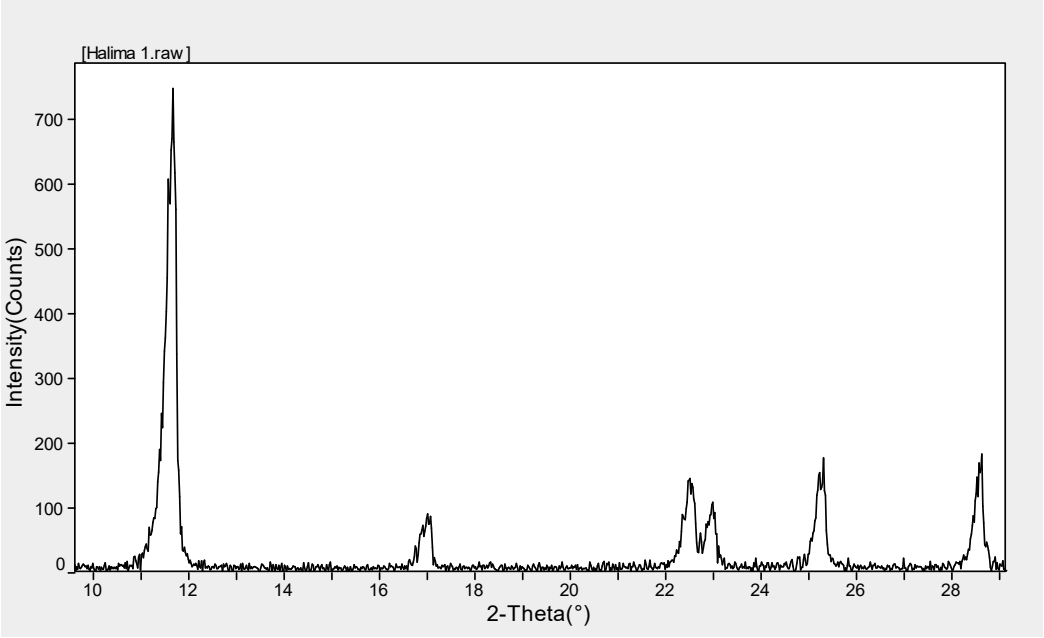

Figure (4.23) XRD spectrum of Talha Gum Arabic doping by Iodiene 0.9 m Molar sample

Table (4.1) Calculate Lattice Constants from Peak Locations and Miller Indices [monoclinic – primitive] of Talha Gum Arabic doping by Iodiene 0.9 m Molar sample

2Ɵ	d (nm)	h k l	Xs(nm)
11.670	7.5739	0 2 0	36.9
17.010	5.2118	1 1 0	45.2
22.509	3.9508	1 1 1	30.5
22.989	3.8694	1 0 1	30.2
25.309	3.5261	1 2 1	56.4
28.623	3.1194	1 3 1	43.0

Average Lattice Constants = 5.929

a= 5.114 b = 15.061 c = 6.517 $\alpha = \beta = \gamma = 90^{O}$

Density = 6.7460 $mg.cm^{-3}$

Crystal Form: Monoclinic – primitive

Space Group: P21/c [14] (Y-unique)

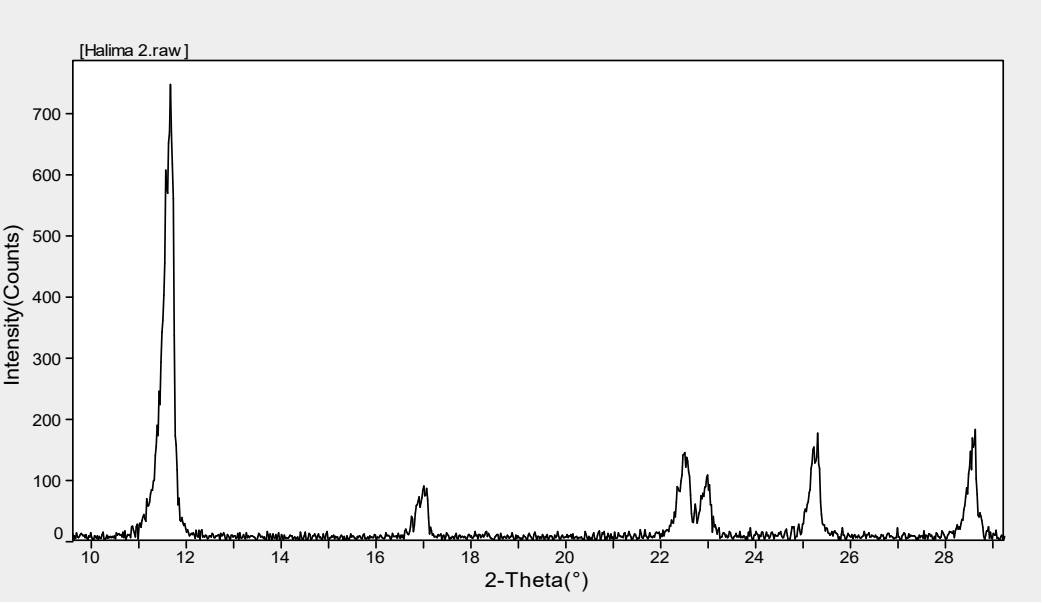

Figure (4.23) XRD spectrum of Talha Gum Arabic doping by Iodiene 0.7 m Molar sample

Table (4.2) Calculate Lattice Constants from Peak Locations and Miller Indices [monoclinic – primitive] of Talha Gum Arabic doping by Iodiene 0.7 m Molar sample

2Θ	d (nm)	h k l	Xs(nm)
11.670	7.6839	0 2 0	34.8
17.010	5.3218	1 1 0	43.2
22.509	4.1308	1 1 1	30.9
22.989	3.9794	1 0 1	29.4
25.309	3.7461	1 2 1	56.5
28.623	3.3494	1 3 1	42.3

Average Lattice Constants = 5.929

a= 5.114 b = 15.061 c = 6.517 $\alpha = \beta = \gamma = 90^{O}$

Density = 6.6350 $mg.cm^{-3}$

Crystal Form: Monoclinic – primitive

Space Group: P21/c [14] (Y-unique)

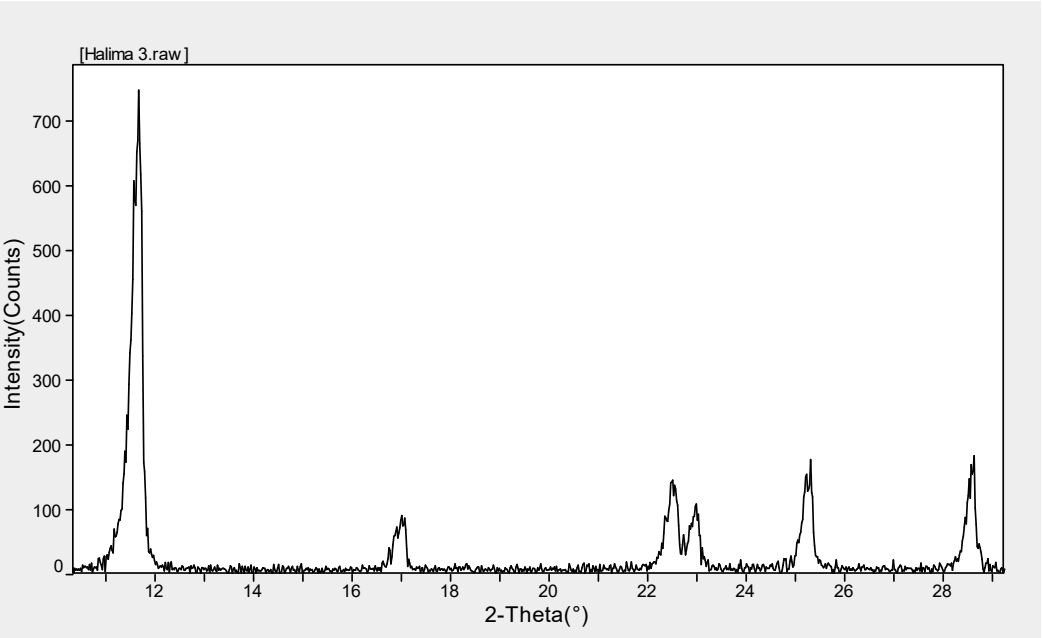

Figure (4.24) XRD spectrum of Talha Gum Arabic doping by Iodiene 0.5 m Molar sample

Table (4.3) Calculate Lattice Constants from Peak Locations and Miller Indices [monoclinic – primitive] of Talha Gum Arabic doping by Iodiene 0.5 m Molar sample

2Ɵ	d (nm)	h k l	Xs(nm)
11.670	7.8939	0 2 0	35.7
17.010	5.5418	1 1 0	43.8
22.509	4.3309	1 1 1	31.3
22.989	4.1194	1 0 1	29.9
25.309	3.9561	1 2 1	57.3
28.623	3.5494	1 3 1	42.8

Average Lattice Constants = 5.929

a= 5.114 b = 15.061 c = 6.517 $\alpha = \beta = \gamma = 90^{O}$

Density = 6.5240 $mg.cm^{-3}$

Crystal Form: Monoclinic – primitive

Space Group: P21/c [14] (Y-unique)

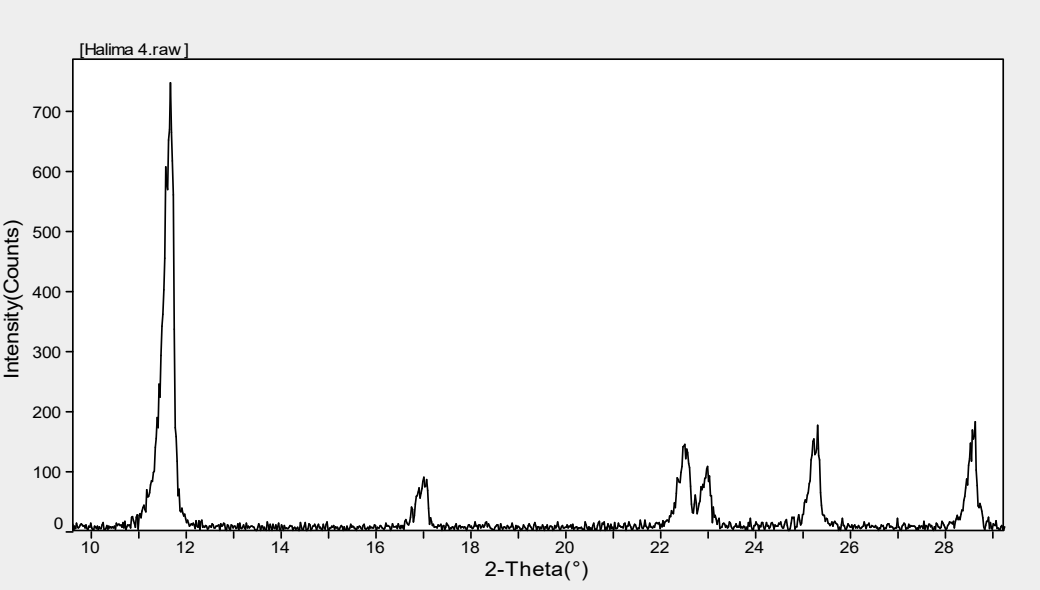

Figure (4.25) XRD spectrum of Talha Gum Arabic doping by Iodiene 0.3 m Molar sample

Table (4.4) Calculate Lattice Constants from Peak Locations and Miller Indices [monoclinic – primitive] of Talha Gum Arabic doping by Iodiene 0.3 m Molar sample

2Ɵ	d (nm)	h k l	Xs(nm)
11.670	7.8939	0 2 0	36.3
17.010	5.5418	1 1 0	44.2
22.509	4.3309	1 1 1	32.5
22.989	4.1194	1 0 1	30.3
25.309	3.9561	1 2 1	57.8
28.623	3.5494	1 3 1	43.4

Average Lattice Constants = 5.929

a= 5.114 b = 15.061 c = 6.517 $\alpha = \beta = \gamma = 90^{O}$

Density = 6.4120 $mg.cm^{-3}$

Crystal Form: Monoclinic – primitive

Space Group: P21/c [14] (Y-unique)

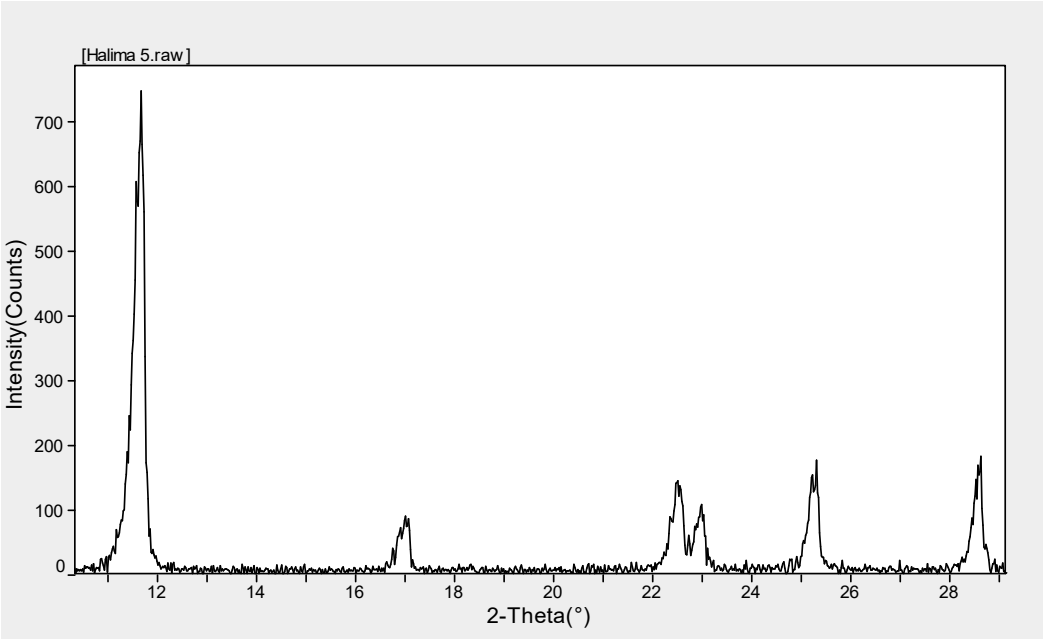

Figure (4.26) XRD spectrum of Talha Gum Arabic doping by Iodiene 0.1 m Molar sample

Table (4.5) Calculate Lattice Constants from Peak Locations and Miller Indices [monoclinic – primitive] of Talha Gum Arabic doping by Iodiene 0.1 m Molar sample

2Θ	d (nm)	h k l	Xs(nm)
11.670	7.8939	0 2 0	36.8
17.010	5.5418	1 1 0	44.7
22.509	4.3309	1 1 1	32.9
22.989	4.1194	1 0 1	30.9
25.309	3.9561	1 2 1	58.3
28.623	3.5494	1 3 1	43.9

Average Lattice Constants = 5.929

a= 5.114 b = 15.061 c = 6.517 $\alpha = \beta = \gamma = 90^{O}$

Density = 6.3110 $mg.cm^{-3}$

Crystal Form: Monoclinic – primitive

Space Group: P21/c [14] (Y-unique)

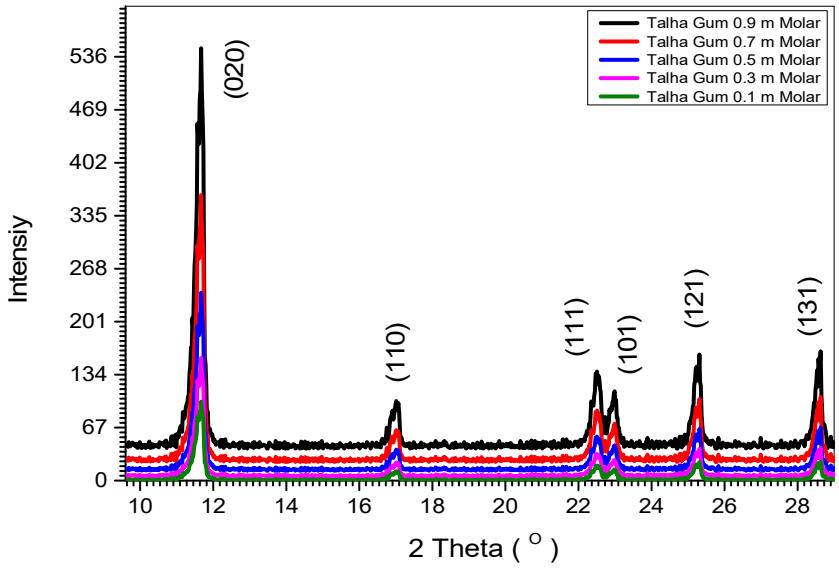

Figure (4.27) XRD spectrum of five Talha Gum Arabic + Iodine samples (0.1, 0.3, 0.5, 0.7 and 0.9) m Molar

Table (4.6) some crystallite lattice parameter (c- form , a,b,c, β,α, γ, density ,Xs(nm) and d – spacing) of five Talha Gum Arabic + Iodine samples (0.1 ,0.3 ,0.5 ,0.7 and 0.9) m Molar

Sample	a	b	c	α= β = γ	Density	Xs(nm)	d-spesing
Hashaba Gum 0.9 m M	5.114	15.061	6.517	90	6.7460	39.14	4.1
Hashaba Gum 0.7 m M	5.114	15.061	6.517	90	6.6350	39.72	4.3
Hashaba Gum 0.5 m M	5.114	15.061	6.517	90	6.5240	40.13	4.5
Hashaba Gum 0.3 m M	5.114	15.061	6.517	90	6.4120	40.32	4.7
Hashaba Gum 0.1 m M	5.114	15.061	6.517	90	6.3110	41.25	4.9

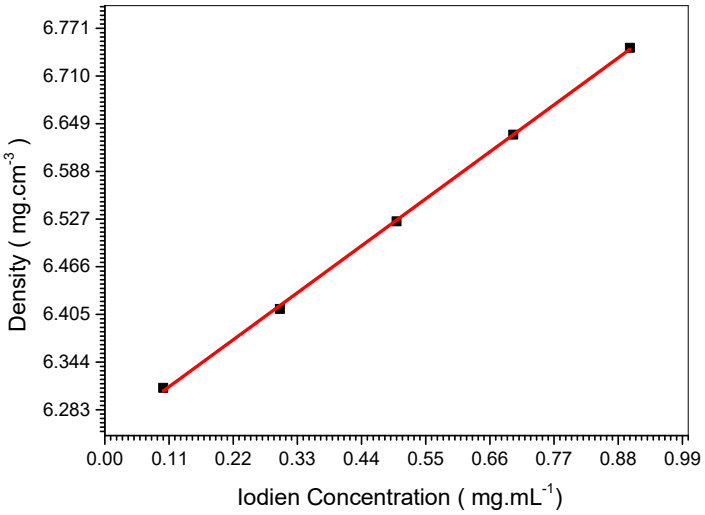

Figure (4.28) relation chip between Iodine concentration and density of five Talha Gum Arabic + Iodine samples (0.1, 0.3, 0.5, 0.7 and 0.9) m Molar

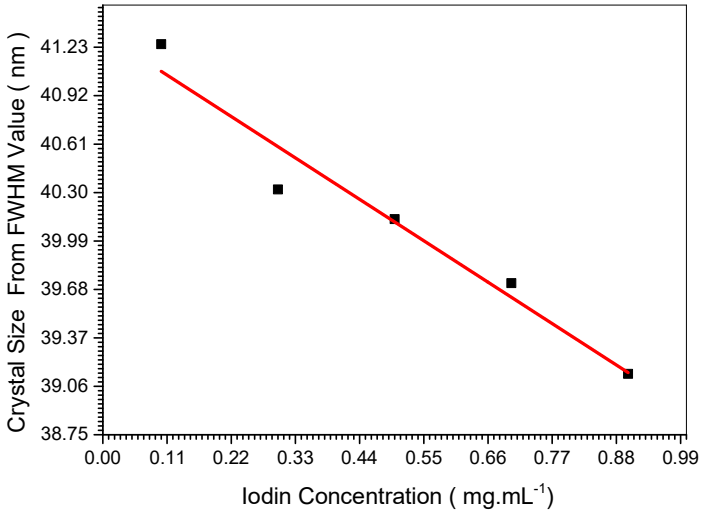

Figure (4.29) relation chip between Iodine concentration and Crystal Size of five Talha Gum Arabic + Iodine samples (0.1, 0.3, 0.5, 0.7 and 0.9) m Molar

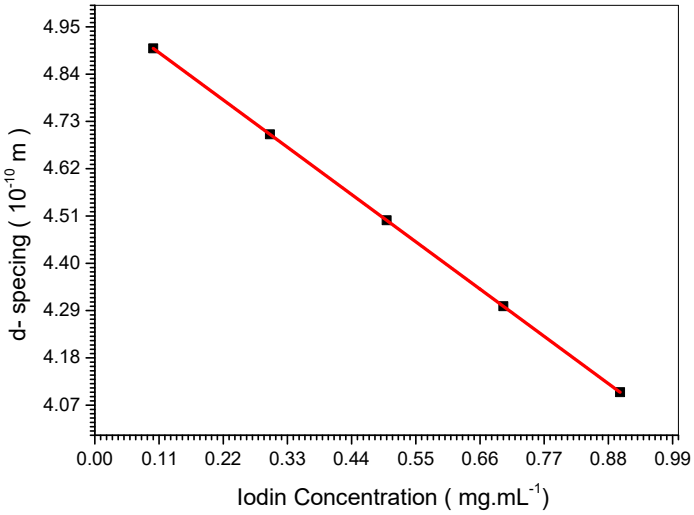

Figure (4.30) relation chip between Iodine concentration and d-specing of five Talha Gum Arabic + Iodine samples (0.1, 0.3, 0.5, 0.7 and 0.9) m Molar.

4.4.1 Discussion of (Talha Gum Arabic + Iodine) samples XRD Results

The crystal structure of all samples characterized at room temperature using a Philips PW1700 X-ray diffractometer (operated at 40 kV and current of 30 mA) and samples were scanned between 10^{O} and 80^{O} at a scanning speed of 0.06 ^{o}C/s using Cu Kα radiation with λ = 1.5418Å. The representative XRD charts of all five Talha GumArabic samples different concentration (0.1,0.30.5,0.7 and 0.9) m Molar as show in fig (4.23) to fig (4.30). Miller indices provided in the figure and all peaks determine transformation of five Talha Gum Arabic samples different concentration (0.1, 0.3, 0.5, 0.7 and 0.9) m Molar crystallites with tetragonal rutile crystal structure. Table (4.1) to table (4.6) shows the XRD parameters of five Talha GumArabic samples different concentration (0.1,0.30.5,0.7 and 0.9) m Molar samples at various crystalline orientations. Fig (4.28) describes the relation between the rated molar of Talha Gum Arabic and Iodine concentration and density of samples, we showing that increase the density of sample by increasing the molar of Iodine samples by rat (0.5465 mg.

Cm-3/molar. The dislocation density (δ) and number of unit cells (n) of Talha Gum Arabic samples different concentration (0.1, 0.3, 0.5, 0.7 and 0.9) m Molar nanoparticles is calculated and listed in table (4.6). Dislocation density decreases and the by number of unit cells increases growth and decreasing the defects in crystallites. Fig (4.29) shows the relation between the rated of Iodene concentration and crystallite size. On the other hand, it's noticed that the rated of Iodene concentration molar increases with decreasing the crystals size by rated 2.41 nm / molar. Finally, fig (4.30) describes the relation between the rated of rated of Iodine concentration and d- spesing of Talha Gum Arabic samples different concentration (0.1,0.30.5,0.7 and 0.9) m Molar nanoparticles samples, and noticed that the rated of decreasing the d- spesing of Talha Gum Arabic samples different concentration (0.1,0.30.5,0.7 and 0.9) m Molar with increases the Iodine concentration molar rated 10^{-10}m / molar.

4.5 XRD Results of (Talha Gum Arabic + Iodine) samples

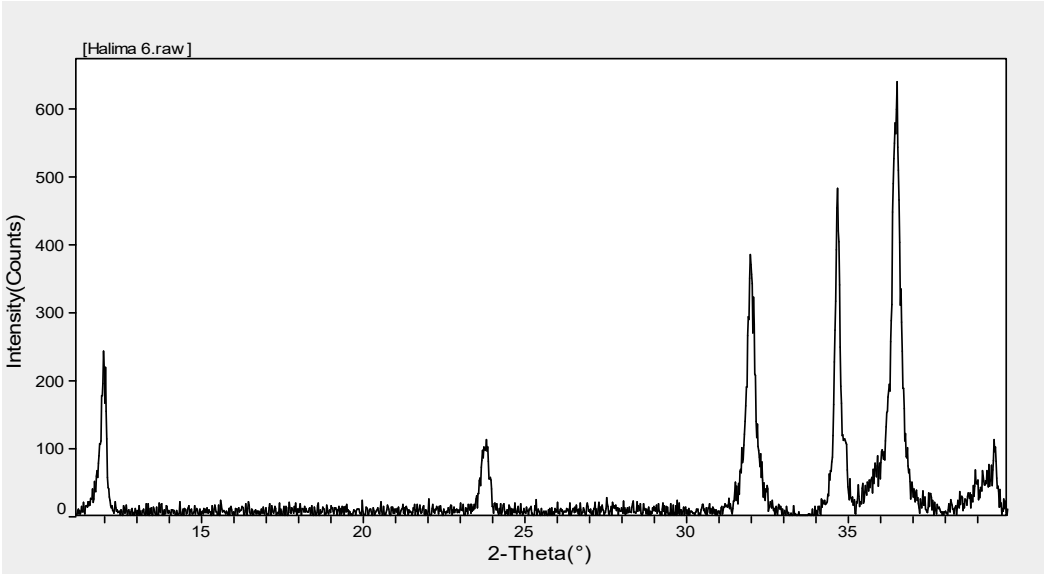

Figure (4.31) XRD spectrum of Hashaba Gum Arabic doping by Iodiene 0.9 m Molar sample

Table (4.7) Calculate Lattice Constants from Peak Locations and Miller Indices [Hexagonal – primitive] of Hashaba Gum Arabic doping by Iodiene 0.9 m Molar sample

2Θ	d (nm)	h k l	Xs(nm)
11.985	7.3642	0 0 3	40.6
23.737	3.7217	0 0 6	31.1
31.974	2.7616	1 1 0	27.7
34.640	2.5316	0 0 2	45.3
36.461	2.4255	1 1 1	26.1
38.974	2.3023	1 0 2	50.1

Average Lattice Constants = 4.4240

a= b = 5.6295 c = 5.6295 $\alpha = \beta = 90^{O}$ $\gamma = 120^{O}$

Density = 3.3986 $mg.cm^{-3}$

Crystal Form: Monoclinic – primitive

Space Group: P6322 (182)

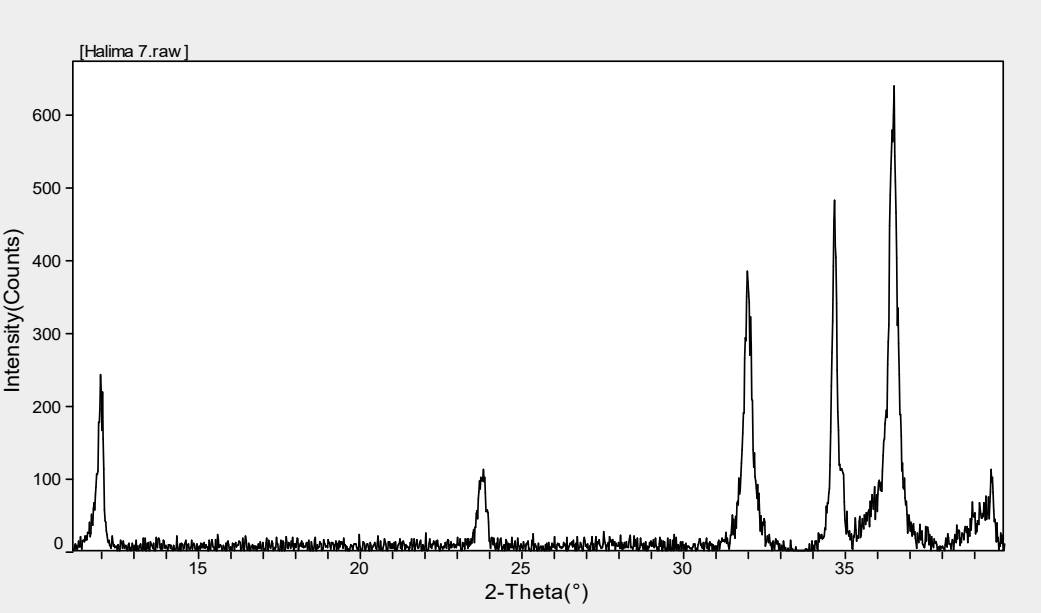

Figure (4.32) XRD spectrum of Hashaba Gum Arabic doping by Iodiene 0.7 m Molar sample

Table (4.8) Calculate Lattice Constants from Peak Locations and Miller Indices [Hexagonal – primitive] of Hashaba Gum Arabic doping by Iodiene 0.7 m Molar sample

2Θ	d (nm)	h k l	Xs(nm)
11.985	7.3653	0 0 3	41.3
23.737	3.7327	0 0 6	31.6
31.974	2.7836	1 1 0	28.2
34.640	2.5446	0 0 2	46.1
36.461	2.4475	1 1 1	26.5
38.974	2.3056	1 0 2	50.6

Average Lattice Constants = 4.4240

a= b = 5.6295 c = 5.6295 $\alpha = \beta = 90^{O}$ $\gamma = 120^{O}$

Density = 3.3775 $mg.cm^{-3}$

Crystal Form: Monoclinic – primitive

Space Group: P6322(182)

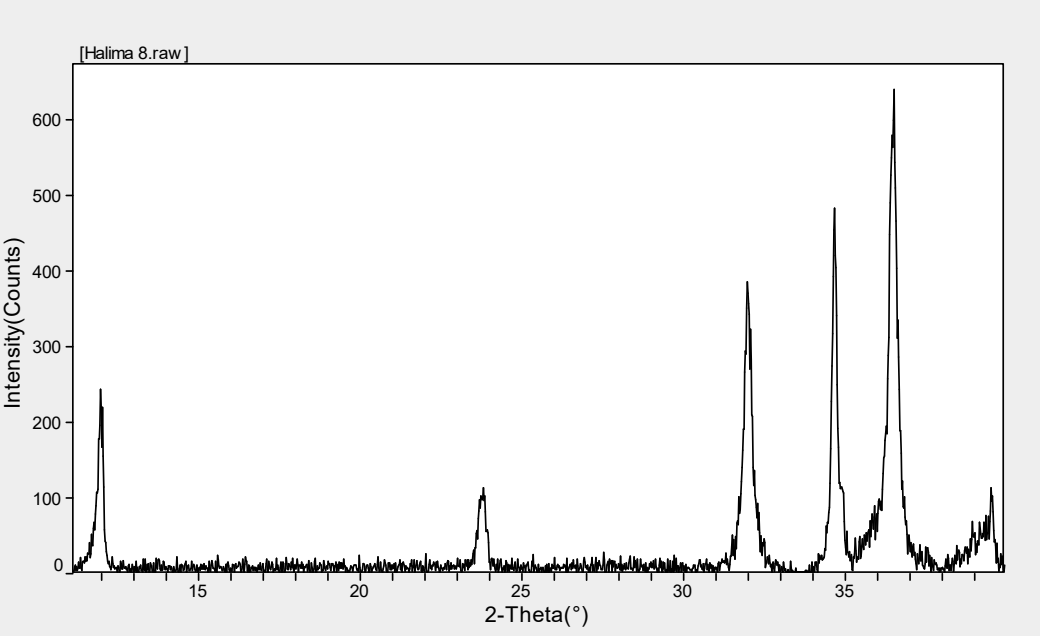

Figure (4.33) XRD spectrum of Hashaba Gum Arabic doping by Iodiene 0.5 m Molar sample

Table (4.9) Calculate Lattice Constants from Peak Locations and Miller Indices [Hexagonal – primitive] of Hashaba Gum Arabic doping by Iodiene 0.5 m Molar sample

2Θ	d (nm)	h k l	Xs(nm)
11.985	7.3664	0 0 3	41.7
23.737	3.7331	0 0 6	32.3
31.974	2.7847	1 1 0	28.7
34.640	2.5452	0 0 2	46.6
36.461	2.4486	1 1 1	27.4
38.974	2.3067	1 0 2	51.2

Average Lattice Constants = 4.4240

a= b = 5.6295 c = 5.6295 $\alpha = \beta = 90^{O}$ $\gamma = 120^{O}$

Density = 3.3593 $mg.cm^{-3}$

Crystal Form: Monoclinic – primitive

Space Group: P6322(182)

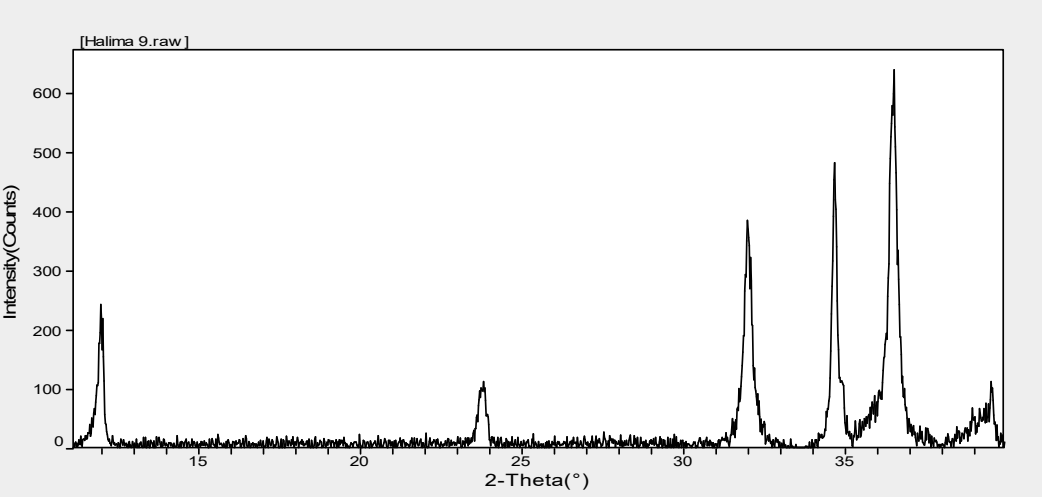

Figure (4.34) XRD spectrum of Hashaba Gum Arabic doping by Iodiene 0.3 m Molar sample

Table (4.10) Calculate Lattice Constants from Peak Locations and Miller Indices [Hexagonal – primitive] of Hashaba Gum Arabic doping by Iodiene 0.3 m Molar sample

2Θ	d (10^{-10}m)	h k l	Xs(nm)
11.985	7.3675	0 0 3	42.8
23.737	3.7342	0 0 6	32.7
31.974	2.7858	1 1 0	29.4
34.640	2.5463	0 0 2	47.3
36.461	2.4497	1 1 1	28.6
38.974	2.3070	1 0 2	52.4

Average Lattice Constants = 4.4240

a= b = 5.6295 c = 5.6295 $\alpha = \beta = 90^{O}$ $\gamma = 120^{O}$

Density = 3.3172 $mg.cm^{-3}$

Crystal Form: Monoclinic – primitive - Space Group: P6322(182)

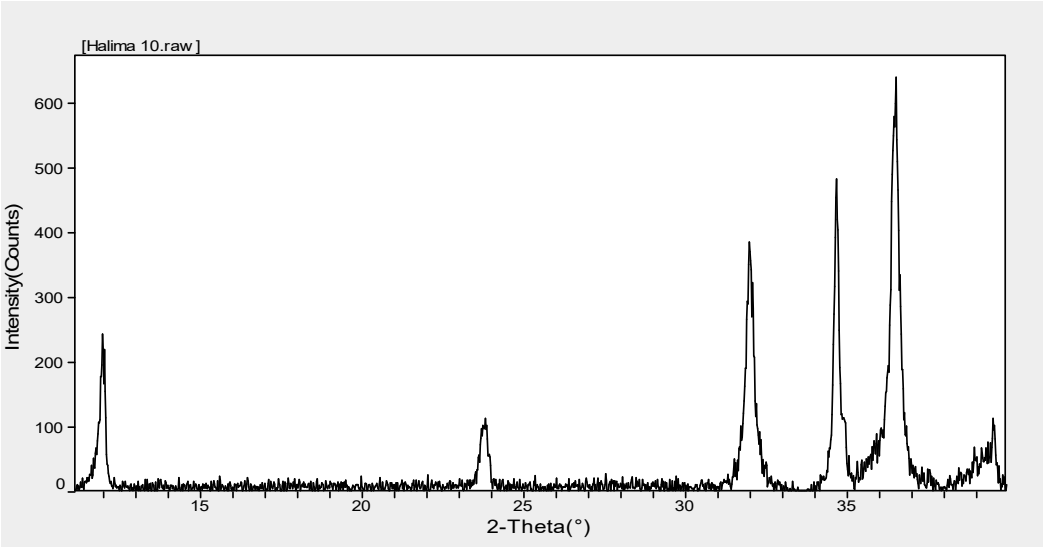

Figure (4.35) XRD spectrum of Hashaba Gum Arabic doping by Iodiene 0.1 m Molar sample

Table (4.11) Calculate Lattice Constants from Peak Locations and Miller Indices [Hexagonal – primitive] of Hashaba Gum Arabic doping by Iodiene 0.1 m Molar sample

2Θ	d (10^{-10}m)	h k l	Xs(nm)
11.985	7.3785	0 0 3	43.4
23.737	3.7452	0 0 6	33.1
31.974	2.7968	1 1 0	29.7
34.640	2.5873	0 0 2	47.9
36.461	2.4607	1 1 1	29.1
38.974	2.3090	1 0 2	53.7

Average Lattice Constants = 4.4240

a= b = 5.6295 c = 5.6295 $\alpha = \beta = 90^{O}$ $\gamma = 120^{O}$

Density = 3.2071 $mg.cm^{-3}$

Crystal Form: Monoclinic – primitive

Space Group: P6322(182)

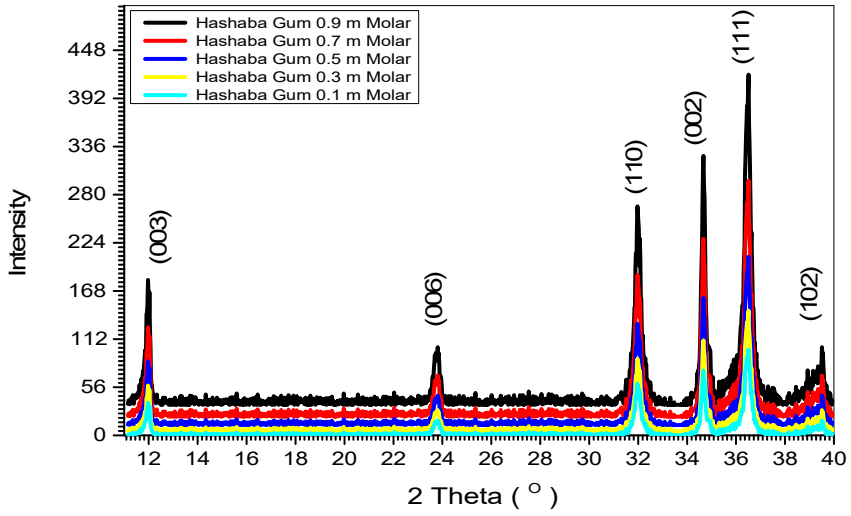

Figure (4.36) XRD spectrum of five Hashaba Gum Arabic + Iodine samples (0.1, 0.3, 0.5, 0.7 and 0.9) m Molar

Table (4.12) some crystallite lattice parameter (c- form , β,α, γ, density ,Xs(nm) and d – spacing) of five Hashaba Gum Arabic + Iodine samples (0.1 ,0.3 ,0.5 ,0.7 and 0.9) m Molar

Sample	α= β	γ	Density	Xs(nm)	d-spesing A^O
Hashaba Gum 0.1 m M	90	120	3.2071	39.5	3.54625
Hashaba Gum 0.3 m M	90	120	3.3172	38.9	3.53175
Hashaba Gum 0.5 m M	90	120	3.3593	37.9	3.530783
Hashaba Gum 0.7 m M	90	120	3.3775	37.4	3.529883
Hashaba Gum 0.9 m M	90	120	3.3986	36.8	3.517817

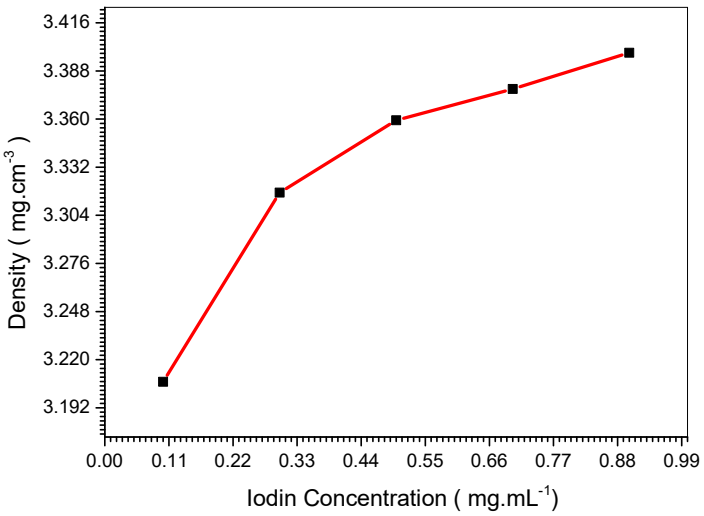

Figure (4.37) relation chip between Iodine concentration and density of five Hashaba Gum Arabic + Iodine samples (0.1, 0.3, 0.5, 0.7 and 0.9) m Molar

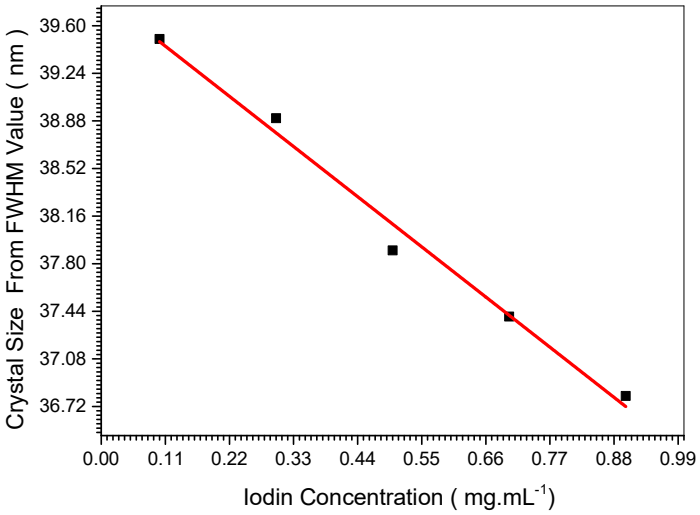

Figure (4.38) relation chip between Iodine concentration and Crystal Size Value of five Hashaba Gum Arabic + Iodine samples (0.1, 0.3, 0.5, 0.7 and 0.9) m Molar

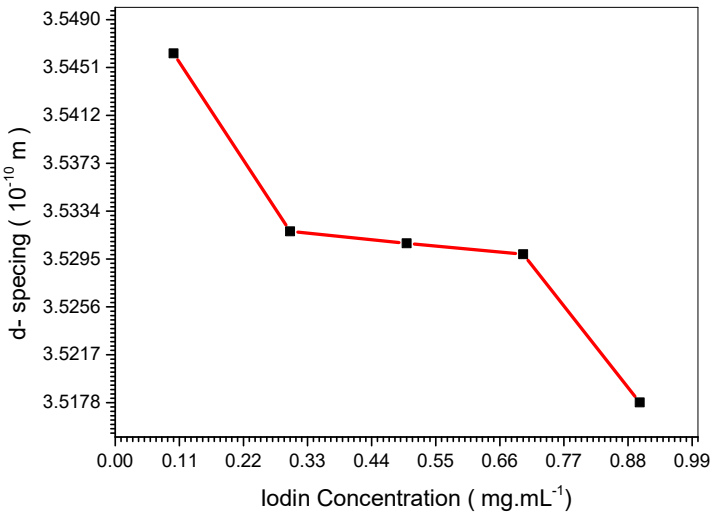

Figure (4.39) relation chip between Iodine concentration and d- Specing of five Hashaba Gum Arabic + Iodine samples (0.1 ,0.3 ,0.5 ,0.7 and 0.9) m Molar

4.5.1 Discussion of (Hashaba Gum Arabic + Iodine) samples XRD Results

The crystal structure of all samples characterized at room temperature using and the same dives that used to characterize Talha Gum Arabic samples. The representative XRD charts of all five Hashaba GumArabic samples different concentration (0.1, 0.3, 0.5, 0.7 and 0.9) m Molar as show in fig (4.31) to fig (4.39). Miller indices provided in the figure and all peaks determine transformation of five Hashaba Gum Arabic samples different concentration (0.1, 0.3, 0.5, 0.7 and 0.9) m Molar crystallites with tetragonal rutile crystal structure. Table (4.7) to table (4.12) shows the XRD parameters of five Hashaba GumArabic samples different concentration (0.1,0.30.5,0.7 and 0.9) m Molar samples at various crystalline orientations. Fig (4.37) describes the relation between the rated molar of Hashaba Gum Arabic and Iodine concentration and density of samples, we showing that increase the density of sample by increasing the molar of Iodine samples by rat 0.2216 mg. Cm-3/molar. The

dislocation density (δ) and number of unit cells (n) of Talha Gum Arabic samples different concentration (0.1, 0.3, 0.5, 0.7 and 0.9) m Molar nanoparticles is calculated and listed in table (4.12). Dislocation density decreases and the by number of unit cells increases growth and decreasing the defects in crystallites. Fig (4.38) shows the relation between the rated of Iodene concentration and crystallite size. On the other hand, it's noticed that the rated of Iodene concentration molar increases with decreasing the crystals size by rated 3.45 nm / molar. Finally, fig (4.39) describes the relation between the rated of rated of Iodine concentration and d- spesing of Hashaba Gum Arabic samples different concentration (0.1,0.30.5,0.7 and 0.9) m Molar nanoparticles samples, and noticed that the rated of decreasing the d- spesing of Hashaba Gum Arabic samples different concentration (0.1,0.30.5,0.7 and 0.9) m Molar with increases the Iodine concentration molar rated 2.93710^{-12}m / molar.

4.5.2 FTIR of (Talha Gum Arabic + Iodine) samples

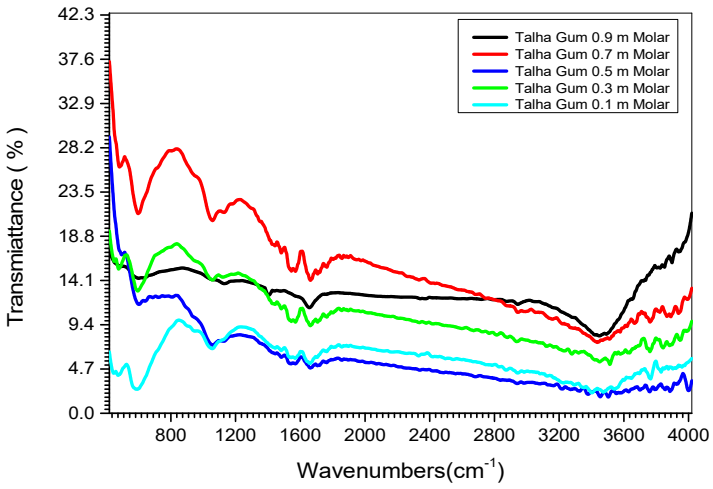

Figure (4.40) FTIR spectrum of five samples Talha Gum Arabic + Iodine by rate (0.1, 0.3, 0.5, 0.7 and 0.9) m Molar

Table (4.13) FTIR wavenumber of five samples Talha Gum Arabic + Iodine by rate (0.1, 0.3, 0.5, 0.7 and 0.9) m Molar

No.	Sample Concentration	υ_1	υ_2	υ_3	υ_4	υ_5	υ_6
1	Talha Gum Arabic 0.9 m Molar	610	1131	1410	1659	2941	3453
2	Talha Gum Arabic 0.7 m Molar	642	1131	1395	1651	2941	3453
3	Talha Gum Arabic 0.5 m Molar	593	1131	1395	1667	2941	3437
4	Talha Gum Arabic 0.3 m Molar	602	1131	1395	1659	2378	3461
5	Talha Gum Arabic 0.1 m Molar	594	1139	1403	1667	2956	3445

The infrared spectra of synthesized fiveTalha Gum Arabic + Iodine by rate (0.1 ,0.3 ,0.5 ,0.7 and 0.9) m Molar nano samples were recorded by mattson Fourier Transform Infrared Spectrophotometer in the range of 400 to 4000 cm^{-1} which shown in Fig(4.40) . The spectra of all samples have been used to locate the band positions which are given in the Table (4.13) . In the present study the absorption bands ν1, ν2, ν3, ν4 , ν5, and ν6 are found to be around 610 cm^{-1}, 1131cm^{-1}, 1410cm^{-1}, 1659cm^{-1}, 2641$cm^{-1}$and 3453cm^{-1} respectively for all the compositions. The transmiattance bands within these specific limits reveal the formation of single-phase spinel structure having two sub-lattices tetrahedral (A) site and octahedral (B) site. The (ν1) band around 610cm^{-1} is caused by the metal-oxygen vibration in the tetrahedral sides. This difference in the spectral positions is due to the different values of metal ion-O^{-2} distances for octahedral and tetrahedral sites. The band (ν2)

around $1131cm^{-1}$ is due to C-C stretch and C-C-H bending. The band (ν3) around 1410 cm^{-1} is associated with the O-H bending vibration .The band (ν4) around 1659 cm^{-1} is due to C=C stretching. (ν5, ν6) around $2641cm^{-1}$and 3453 cm^{-1} is due to the stretching mode of H-O-H bending vibration of free or absorbed water which implies that the hydroxyl groups are retained in ferrites .

4.5.3 FTIR of (Hashaba Gum Arabic + Iodine) samples

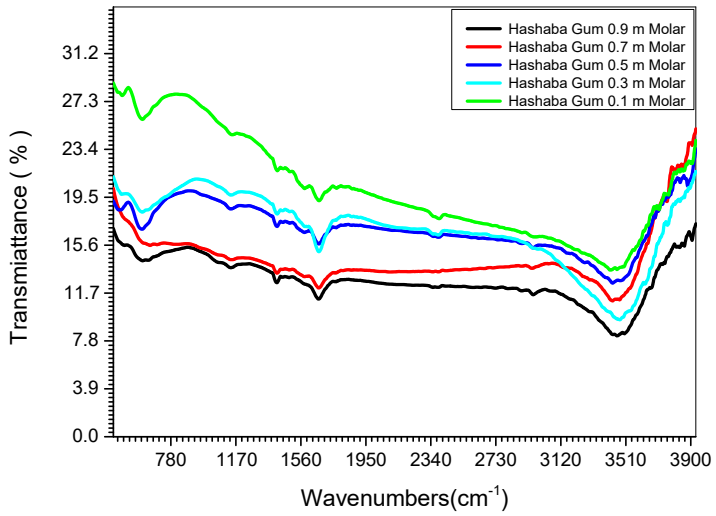

Figure (4.41) FTIR spectrum of five samples Hashaba Gum Arabic + Iodine by rate (0.1, 0.3, 0.5, 0.7 and 0.9) m Molar.

Table (4.14) FTIR wavenumber of five samples Hashaba Gum Arabic + Iodine by rate (0.1, 0.3, 0.5, 0.7 and 0.9) m Molar

No.	Sample Concentration	υ_1	υ_2	υ_3	υ_4	υ_5	υ_6
1	Hashaba Gum Arabic 0.9 m Molar	623	1141	1415	1670	2952	3460
2	Hashaba Gum Arabic 0.7 m Molar	495	605	1141	1570	1680	3454
3	Hashaba Gum Arabic 0.5 m Molar	605	1141	1555	1685	3408	
4	Hashaba Gum Arabic 0.3 m Molar	480	605	1141	1560	1675	3520
5	Hashaba Gum Arabic 0.1 m Molar	480	605	1141	1570	1675	3470

The infrared spectra of synthesized five samples Hashaba Gum Arabic + Iodine by rate (0.1 ,0.3 ,0.5 ,0.7 and 0.9) m Molar nano samples were recorded by mattson Fourier Transform Infrared Spectrophotometer in the range of 400 to 4000 cm^{-1} which shown in Fig(4.41) . The spectra of all the ferrites have been used to locate the band positions which are given in the Table (4.14) . In the present study the absorption bands ν1, ν2, ν3, ν4 , ν5, and ν6 are found to be around 623 cm^{-1}, 1141cm^{-1}, 1415cm^{-1}, 1670cm^{-1}, 2952$cm^{-1}$and 3460cm^{-1} respectively for all the compositions. The transmiattance bands within these specific limits reveal the formation of single-phase spinel structure having two sub-lattices tetrahedral (A) site and octahedral (B) site. The (ν1) band around 480 - 612 cm^{-1} is caused by the metal-oxygen vibration in the tetrahedral sides. This difference in the spectral positions is due to the different values of metal ion-O^{-2} distances for octahedral and tetrahedral sites.

The band (ν2) around $1141\ cm^{-1}$is due to C-C stretch and C-C-H bending. The band (ν3) around $1415\ cm^{-1}$ is associated with the O-H bending vibration .The band (ν4) around $1670\ cm^{-1}$ is due to C=C stretching. (ν5, ν6) around $2952\ cm^{-1}$and $3460\ cm^{-1}$ is due to the stretching mode of H-O-H bending vibration of free or absorbed water which implies that the hydroxyl groups are retained in ferrites .

CHAPTER FIVE

CONCLUSION AND RECOMMENDATION

5.1 Conclusion

For samples of Carbon doping by Aluminum Oxide, the rapid increase of absorption at wavelengths 235 nm corresponding photon energy 5.277 eV by doping increase, also show that absorbance value increase when the molar of Aluminum Oxide increase, and for Carbon doping by Iron Oxide, the rapid increase of an absorption at wavelengths 375 nm corresponding photon energy 3.307 eV also show that absorbance value increase by doping increase to.

For absorption coefficient the value of the samples of Carbon doping by Aluminum Oxide 0.9 Molar equal $4.99x10^4$ cm^{-1} in the U.V region (235 nm) but for sample 0.1 Molar sample equal $2.41x10^4$ cm^{-1} at the same wavelength, and for the Carbon doping by Iron Oxide 0.9 molar equal $3.19x10^4$ cm^{-1} in the U.V region (375 nm) but for sample 0.1 Molar equal $1.54x10^4$ cm^{-1} at the same wavelength. For the absorption coefficient of all Carbon doping by (Aluminum, Iron) Oxide samples the transition must be corresponding to a direct electronic transition, and the properties of this state are important since they are responsible for electrical conduction. Also, the value of absorption coefficient of Carbon doping by (Aluminum, Iron) Oxide samples increase while doing increased. Refractive index (n) spectra of prepared samples by Carbon doping by Aluminum Oxide the maximum value is (2.134) for sample 0.9 Molar at 300 nm wavelength but for 0.1 Molar sample equal 1.031 at the same wavelength , but for the prepared sample by Carbon doping by Iron Oxide the refractive index (n) maximum value is (2.152) for all samples at tow point of spectrum the first point at wavelength ranged (200 to 245) nm, and the second point at (500 -545) nm wavelength ,the second point was agreement with red shift by increase for Iron Oxide doping ,but the first was blue shift .

The value of Energy Band Gap (Eg) of Carbon doping by Aluminum Oxide 0.9 Molar sample obtained was (3.376) eV while for other sample Carbon doping by Aluminum Oxide 0.1 Molar sample obtained was (3.505) eV. And Carbon doping by Iron Oxide 0.9 Molar sample obtained was (2.264) eV while for other sample Carbon doping by Iron Oxide 0.1 Molar sample obtained was (2.409) eV. The value of(Eg) was decreased from (3.505) eV to (3.376) eV for Carbon doping by Aluminum Oxide and decreased from (2.409) eV to (2.264) eV for Carbon doping by Iron Oxide sample, The decreasing of (Eg) related to increase of (Aluminum or Iron) Oxide molar on the samples. It was observed that the different (Aluminum or Iron) Oxide molar for Carbon confirmed the reason for the band gap shifts.

Crystal crystallites with Carbon doping by Aluminum Oxide are (Hexagonal - primitive), but for the Carbon doping by Iron Oxide samples are (Orthorhombic- primitive) crystal structure.

Describes the relation between the rated molar of Carbon and (Aluminum or Iron) Oxide concentration and density of all samples, we showing that increase the density of sample by increasing the molar of (Aluminum or Iron) Oxide samples by rat (0.8572 mg. cm^{-3}/mole) for Aluminum oxide and (0.5103 mg. cm^{-3}/mole) for the Iron Oxide.

For the relation between the rated of (Aluminum or Iron) Oxide concentration and crystallite size we show that Aluminum Oxide concentration molar increases with decreasing the crystals size by rated 31.025 nm / molar, and Iron Oxide concentration molar increases with decreasing the crystals size by rated 14.73 nm / molar.

Finally describes the relation between the rated of rated of (Aluminum or Iron) Oxide concentration and d- spesing of Carbon doping by (Aluminum or Iron) Oxide samples rated (0.1 ,0.3 ,0.5 ,0.7 and 0.9) Molar nanoparticles samples, and noticed that the rated of decreasing the d- spesing of Carbon doping by Aluminum Oxide with increases the Aluminum Oxide concentration molar

rated $0.28085x10^{10}$ m / molar and for Iron Oxide samples increases the Iron Oxide concentration molar by rated 17.158^{-12} m / molar.

5.2 Recommendation

- The Study recommended to study sufficient studies to determine other optical properties.
  - Studying the optical properties by other devices and using the method of chemical analysis and increasing the concentration or used other oxide and studying its electrical properties.
  - Studying this material by other dives like (FTIR- spectroscopy, SEM or TEM).
  - Use this material on any application.

References

[1] Abdel Magid, A. A., 2014. Book review “Gum Arabic in the Sudan Sudan Vision” (unpublished).

[2] Abdel Magid, T.D., Eltayb, M.T.A., Dirar, A.M.A., 2014. Equalizing gum codal term (a Code E414), of Acacia senega1 (L) with Acacia seyal (Del.), and its impact on gum production and exportation. J. App. Ind. Sci. 2 (3), 144–151.

[3] Abdelnour, H.O., 1999. Gum Arabic in Sudan: production and socio-economic aspects: medicinal culinary and aromatic plants in the near east. In: Proceedings of the International Expert Meeting organized by the Forest Products Division. FAO Forestry Department andthe FAO Regional Office for the Near East, Cairo, Egypt.

[4] Abdulgadir, A., 2013. Secretary General of the Gum Arabic Council. Available from: http:// news.sudanvisiondaily.com/details.html.

[5] Adam, A.A., 2013. Effects of grass burning, tree size and tapping on gum talha (Acacia seyal Del. var. seyal) yield in South Kordofan State. MSc. Thesis, University of Kordofan.

[6] Ahmed, M.E., 2006. The socio-economic role of Acacia senegal in sustainable development of rural area in the gum belt of the Sudan. Institut für Internationale Forst- und Holzwirtschft, Technische Universitۤt Dresden, Tharandt, Germany.

[7] Ali, E. Y., 2006. Yield Potential of Acacia seyal Del. variety seyal in Relation to Growth Parameters, Methods and Position of Tapping. MSc. Thesis, University of Kordofan.

[8] Anderson, D.M., Bridgeman, M.M., De Pinto, G., 1984. Acacia gum exudates from species of the series gummiferae. Phytochemistry, 575–577.

[9] Badi, K.H.M., Ahmed, A.E., Bayoumi, A.M.S., 1989. The Forests of the Sudan. Khartoum Agricultural Research Council, Sudan.

[10] Ballal, M. E., 2002. Yield Trends of Gum Arabic from Acacia senegal as Relation to Some Environmental and Managerial Factors (PhD Thesis), Faculty of Forestry, University of Khartoum.

[11] Barbier, E.B., 1992. Rehabilitating gum Arabic systems in Sudan: economic and environmental implications. Environ. Resour. Econ. 2 (4), 341–358.

[12] Beyene, M., 1993. Investing in Acacia senegal lessons from the Sudanese experience to Eritrea. African Arid Lands Working Paper Series No. 4/93.

[13] Central Bank of Sudan, Annual reports (2002–2014). Available from: http://www.cbos.gov.sd.

[14] Chikamai, B., 1997. Production, markets and quality control of gum Arabic in Africa: findings and recommendations from an FAO project. In: Mugah, J.O., Chikamai, B.N., Mbiru,

[15] S.S., Casad, E. (Eds.), Conservation, Management and Utilization of Plant Gums, Resins and Essential Oils. Forestry Department, FAO, Proceedings of a regional conference for Africa, October 6–10, 1997. FAO, Rome, Nairobi, Kenya.

[16] Dorthe, J., 2000. Acacia senegal (L) Wild Seed Leaflet. Danida Forest Seed Center, Denmark, No. 5, 1–2.

[17] Eisa, M.A., Roth, M., Sama, G., 2008. *Acacia Senegal* (Gum Arabic Tree): Present role and need for future conservation/Sudan. Paper presented on Deutscher Tropentag, Germany.

[18] Eldukheri, I. A. 1997. Past Changes and Future Prospects of Traditional Rain-fed Farming in North Kordofan State. Ph.D Dissertation, Technical University of ünchen, Germany.

[19] Elkhidir, E.E., Zubaidi, B.A.S., Shzee, Y.T., 2010. Estimation of technical efficiency for share contract of producing gum Arabic: Kordofan gum Arabic belt, Sudan. Res. J. Forest. 4, 185–193.

[20] Elmqvist, B., Olsson, L., Elamin, E.M., Warren, A., 2005. A traditional agroforestry system under threat: an analysis of the gum Arabic market and cultivation in the Sudan. Agroforest Syst. 64, 211–218.

[21] Elsiddig, E.A., 2003. Aboveground wood weight and volume relationships for *Acacia seyal* in Eastern Sudan. Sudan Silva 9 (1), 25–39.

[22] Elsiddig, E.A., Abdel Magid, D.A., 2007. Sudan forestry sector review. In: Abdelnour, H.O.(Ed.), Forests National Corporation. National Forest Programme, Khartoum, Sudan.

[23] Elsiddig, E.A., Elballal, M.E., Abdel Magid, T.D., 2005. The *Acacia senegal* agroforestry system in the Sudan. In: Proceedings of the Planary Garden workshop. Brazil, September 26–28.

[24] Fadl, K.M., Gebauer, J., 2004. Effect of different tapping tools and different tapping positions on “talh gum” yield of Acacia seyal var. seyal in South Kordofan, Sudan. Conference on International Agricultural Research for Development. Berlin, October 5–7, 2004.

[25] Hall, J.B., McAllan, A., 1993. Acacia seyal: A Monograph. School of Agricultural and Forest Sciences, University of Wales, Bangor, UK.

[26] Hammad, Z.M., 2014. Transformations in Agroforestry Systems in the Gum Belt of Kordofan. LAP LAMBERT Academic Publishing, Germany.

[27] Hineit, B.M., 2007. Effect of Type, Time of Tapping and Tree Size of Acacia seyal var. seyal on the Production of Gum Talha in Rawashda forest (Master Thesis). Faculty of Forestry, University of Khartoum, Gedarif State, Sudan.

[28] ILO, Intensive Labour Organization, 1985. Project Identification mission 1984, Ministry of Agriculture, Sudan.

[29] Iqbal, M., 1993. International Trade in Non-wood Forest Products: An Overview. FAO, Rome, FO: Misc/93/11 Working Paper.

[30] Jamal, A., 1994. Major insect pests of gum Arabic Acacia Vild and *Acacia seyal* (L) in Western Sudan. J. Appl. Entomol. 117 (1), 10–20.

[31] JECFA, (FAO/WHO) Expert Committee on Food Additives, 1999. Compendium of Food Additive Specifications. Appendum 7, Joint JECFA 53rd session June 1–10, Rome.

[32] Karama, M., 2002. Gum Arabic Marketing Issues: Marketing Model, Buffer-Stocking, Processing and Finance. Unpublished Paper Presented by the International Workshop on Promotion of Gum Arabic Production, Processing and Marketing, Khartoum, Sudan.

[33] Larson, B.A., Bromley, D.W., 1991. Natural resource prices, export policies, and deforestation: the case of Sudan. World Develop. 19 (10), 1289–1297.

[34]Macrae, J., Merlin, G., 2002. The prospects and constraints of development of gum Arabic in Sub-Saharan Africa. World Bank, Washington, D.C.

[35] Mohammed, M.H., 2011. Management of natural stands of *Acacia seyal* Del. variety *seyal* (Brenan) for production of gum *talha*, South Kordofan, Sudan. TUDpress, Verlag der Wissenschaften GmbH, Dresden.

[36] McAllan, A., 1993. Acacia Seyal: a Handbook for Extension Workers. School of Agricultural and Forest Sciences, University of Wales, Bangor, UK.

[37] Montagnini, F., Cusack, D., Petit, B., Kanninen, M., 2005. Environmental Services of Native Tree Plantations and Agroforestry Systems in Central

America. The Haworth Press, Inc., doi:10.1300/J091v21n01_03; http://www.haworthpress.com/web/JSF.

[38] Mustafa, A.F., 1997. Regeneration of *Acacia seyal* Forests on the Dryland of the Sudan Clay Plain: Tropical Forestry Report No. 15. Department of Forest Ecology, Helsinki University Printing House, Helsinki NAS, National Academy of Sciences, 1979. Tropical Legumes: Resources for the Future. NAS, Washington, D.C.

[39] NEF, Near East Foundation, 2010. NEF Launches Gum Arabic Project in Central Sudan. Oba, G., Stenseth, N.C., Weladji, R.B., 2002. Impacts of shifting agriculture on a floodplain woodland regeneration in dry-land, Kenya. Agric. Eco. Environ. 90, 211–216.

[40] Olsson, K., 1984. Long-term Changes in Woody Vegetation in the North Kordofan—the Sudan: A Study with Special Emphasis on *Acacia senegal*. Lund University, Lund, Sweden.

[41] Pearce, D., Barbier, E., Avil, M., 1990. Sustainable Development: Economics and Environment in the Third World. Edward Elgar Publ. Ltd, Aldershot, England.

[42] Pretzsch, J., Taha, M.E., Siddig, M.E., Dafalla, T.H.H., Elamin, H.M.A., 2014. Valuation of environmental role of Acacia senegal Tree in the gum belt of Kordofan and the Blue Nile

[43] Nasif, W., Lotfy, M., Mahmoud, M., 2011. Protective effect of gum acacia against the aspirin induced intestinal and pancreatic alterations. Eur. Rev. Med. Pharmacol. Sci. 15, 285–292.

[44] Nasir, O., Wang, K., Föller, M., Bhandaru, M., Sandulache, D., Artunc, F., Ackermann, T.F., Ebrahim, A., Palmada, M., Klingel, K., 2010. Downregulation of angiogenin transcript levels and inhibition of colonic carcinoma by Gum Arabic (*Acacia senegal*). Nutr. Cancer 62, 802–810.

[45] Nordin, N., Salama, S.M., Golbabapour, S., Hajrezaie, M., Hassandarvish, P., Kamalidehghan,

[46] B., Majid, N.A., Hashim, N.M., Omar, H., Fadaienasab, M., 2014. Anti-ulcerogenic effect of methanolic extracts from *Enicosanthellum pulchrum* (King) Heusden against ethanolinduced acute gastric lesion in animal models. PLoS One 9, e111925.

[47] Pal, R., Hooda, M., Bhandari, A., Singh, J., 2012. Antioxidant potential and free radicals scavenging activity by pod extracts of *Acacia senegal* willd. Int. J. Pharm. Chem. Biol. Sci. 2, 500–506.

[48] Pope, J.L., Tomkovich, S., Yang, Y., Jobin, C., 2017. Microbiota as a mediator of cancer progression and therapy. Transl. Res. 179, 139–154.

[49] Qader, S.W., Abdulla, M.A., Chua, L.S., Sirat, H.M., Hamdan, S., 2012. Pharmacological mechanisms underlying gastroprotective activities of the fractions obtained from *Polygonum minus* in sprague dawley rats. Int. J. Mol. Sci. 13, 1481–1496.

[50] Repetto, M., Llesuy, S., 2002. Antioxidant properties of natural compounds used in popular medicine for gastric ulcers. Braz. J. Med. Biol. Res. 35, 523–534.

[51] Robins, P., 1980. Ultrastructural observations on the pathogenesis of aspirin-induced gastric erosions. Br. J. Exp. Pathol. 61, 497–504.

[52] Rodrigues, R., Jorge, M., Sousa, I.D.O., Lima, J., Ruiz, A., Carvalho, J., Figueira, G., Foglio,

[53] M., 2009. Pharmacological activity from Arrabidaea Chica Verlot bioencapsulated with arabic gum. XVIIth International Conference on Bioencapsulation, Groningen, Netherlandspp. 24–26.

[54] Salama, S.M., Gwaram, N.S., Alrashdi, A.S., Khalifa, S.A., Abdulla, M.A., Ali, H.M., EL-seedi, H.R., 2016. A zinc morpholine complex prevents

HCl/ethanol-induced gastric ulcers in a rat model. Sci. Rep. 6doi: 10.1038/srep29646.

[55] Shimoyama, S., Kaminishi, M., 2000. Increased angiogenin expression in gastric cancer correlated with cancer progression. J. Cancer Res. Clin. Oncol. 126, 468–474.

[56] Sidahmed, H., Abdelwahab, S.I., Mohan, S., Abdulla, M.A., Taha, M.M.E., Hashim, N.M.,

[57] Hadi, A.H.A., Vadivelu, J., Loke Fai, M., Rahmani, M., 2013. α-Mangostin from Cratoxylum arborescens (Vahl) Blume demonstrates anti-ulcerogenic property: a mechanisticstudy. Evid. Based Complement. Altern. Med. 2013doi: 10.1155/2013/450840.

[58] H. Mustafa, R.AbdElgani, A. Suliman, A.M.Ahmed4, Amal A.Abdallah, Asma Mohammed & Sawsan Ahmed Elhouri Ahmed- Improving The Properties Of Gum Arabic To Act As Semiconductor -Global Journal Of Engineering Science And Researches-[Mustafa, 2(11): November 2015] ISSN 2348 – 8034 - Impact Factor- 3.155 .

[59] Siddig T. Kafi, Murwan. K. Sabahalkhair - Effects of ã-Irradiation on Some Properties of Gum Arabic *(Acacia Senegal L)* - Research Journal of Agriculture and Biological Sciences, 6(2): 113-117, 2010 © 2010, INSInet Publication .

[60] Elhadi M. I. Elzain, Lyla Mobarak, Mobarak Dirar - Investigating the Electric Conductivity, Magnetic Inductivity, and Optical Properties of Gum Arabic Crystals - Journal of Basic and Applied Chemistry, 2(6)35-49, 2012 © 2012, Text Road Publication ISSN 2090-424X www.textroad.com .

[61] J. K. Lelon1*, I. O. Jumba2, J. K. Keter2, Wekesa Chemuku and F. D. O. Oduor2 - Assessment of physical properties of gum arabic from *Acacia senegal* varieties in Baringo District, Kenya - African Journal of Plant Science Vol. 4(4), pp. 95-98, April 2010 Available online at

http://www.academicjournals.org/ajps ISSN 1996-0824 © 2010 Academic Journals .

[62] Moses M. Solomona,⋆, Husnu Gerengia, Saviour A. Umorenb, Nsikak B. Essienc, Uduak B. Essienc, Ertugrul Kayaa - Gum Arabic-silver nanoparticles composite as a green anticorrosive formulation for steel corrosion in strong acid media - journal homepage: www.elsevier.com/locate/carbpol - Carbohydrate Polymers 181 (2018) 43–55 .

[63] S. L. Elliott, R. F. Broom, and C. J. Humphreys[a]) - Dopant profiling with the scanning electron microscope-A study of Si - JOURNAL OF APPLIED PHYSICS VOLUME 91, NUMBER Il 1 JUNE 2002.

[64] Yolanda L. López-Franco a, Raúl E. Córdova-Moreno a, Francisco M. Goycoolea a,1, Miguel A. Valdez b, Josue Juárez-Onofre b, Jaime Lizardi-Mendoza a,* - Classification and physicochemical characterization of mesquite gum (Prosopis spp.) - journal homepage: www.elsevier.com/locate/foodhyd - Food Hydrocolloids 26 (2012) 159e166 .

[65] D. Bhakat, P. Barik 1, A. Bhattacharjee * - Electrical conductivity behavior of Gum Arabic biopolymer-Fe3O4 nanocomposites - Journal of Physics and Chemistry of Solids - journal homepage: www.elsevier.com/locate/jpcs - Journal of Physics and Chemistry of Solids 112 (2018) 73–79 .

[66] Elkhatem Elmhdy Ali Mohamed - Dr. Mahmoud Hamid Mahmoud Hilo - Determination of the Energy Gap of Gum Arabic Doped with Zinc Oxide Using the UV-VIS Technique - A dissertation Submitted in a partial fulfillment of the Requirements of M.Sc. degree in Physics- Sudan University of Science & Technology College of Postgraduate Studies - Aug- 2018.

[67] Susana I. C. J. Palmaa, Alexandra Carvalhob, Joana Silvac, Pedro Martinsc, Marzia Marciellod, Alexandra R. Fernandesc,e, Maria del Puerto Moralesd and Ana C. A. Roquea - Covalent coupling of gum arabic onto superparamagnetic iron oxide nanoparticles for MRI cell labeling:

physicochemical and in vitro characterization - Contrast Media Mol. Imaging (2015) Copyright © 2015 John Wiley & Sons, Ltd. wileyonlinelibrary.com . DOI: 10.1002/cmmi.1635.

[68] PUSPENDU BARIK, ASHIS BHATTACHARJEE, and Madhusudan Roy- Preparation, characterization and electrical study of gum arabic/ZnO nanocomposites - Bull. Mater. Sci., Vol. 38, No. 6, October 2015, pp. 1609–1616. c_ Indian Academy of Sciences.

[69] Abdelsakhi .S.M - Using Gum Arabic in Making Solar Cells by Thin Films Instead Of Polymers - IOSR Journal of Applied Physics (IOSR-JAP) ISSN: 2278-4861.Volume 8, Issue 1 Ver. III (Jan. - Feb. 2016), PP 27-32.

[70] Mubarak Dirar Abd-alla – Alobid Ali Khalid Awad Elkareem - Mohammed Idriss Ahmed- Abdalsakhi .S .M.H - Rawia Abd Elgani . The Effect of Optical Energy Gaps on the Efficiency for Dye Sensitized Solar Cells (DSSC) by using Gum Arabic Doped by CuO and (Coumarin 500, Ecrchrom Black, Rhodamin B and DDTTc) Dyes-IJISET - International Journal of Innovative Science, Engineering & Technology, Vol. 6 Issue 12, December 2019 ISSN (Online) 2348 – 7968 | Impact Factor (2019) – 6.248 www.ijiset.com .